Long-range transport of Asian outflow to the equatorial Pacific

Brian D. Martin,[1] Henry E. Fuelberg,[1] Nicola J. Blake,[2] James H. Crawford,[3] Jennifer A. Logan,[4] Donald R. Blake,[2] and Glen W. Sachse[3]

Received 23 October 2001; revised 6 February 2002; accepted 12 February 2002; published 5 December 2002.

[1] The second Pacific Exploratory Mission to the Tropics (PEM T-B) was conducted as part of NASA's Global Tropospheric Experiment (GTE) from 25 February through 19 April 1999. Long-range pollution signatures are examined during four PEM T-B flights that ranged as far northeast as California and as far southwest as coastal New Guinea. The signatures are studied to determine their ages and chemical evolution during transport. The chemical species examined include nonmethane hydrocarbons, halocarbons, and carbon monoxide. Wind data from the European Centre for Medium Range Weather Forecasts (ECMWF) are used to calculate backward trajectories along the four flight tracks. Results show that some pollutants originating from the Asian continent, and even farther west, are transported across the Pacific by the middle latitude westerly winds and reach the subtropical Pacific anticyclone where they subside and turn southwestward under the influence of the low level trade winds. The parcels ultimately reach the western Pacific near coastal New Guinea after 20–25 days of transit. *INDEX TERMS:* 0368 Atmospheric Composition and Structure: Troposphere—constituent transport and chemistry; 3319 Meteorology and Atmospheric Dynamics: General circulation; 3364 Meteorology and Atmospheric Dynamics: Synoptic-scale meteorology; 3374 Meteorology and Atmospheric Dynamics: Tropical meteorology

Citation: Martin, B. D., H. E. Fuelberg, N. J. Blake, J. H. Crawford, J. A. Logan, D. R. Blake, and G. W. Sachse, Long-range transport of Asian outflow to the equatorial Pacific, *J. Geophys. Res.*, *107*, 8322, doi:10.1029/2001JD001418, 2002. [printed *108*(D2), 2003]

1. Introduction

[2] Asia currently has 3.4 billion people, 60% of the world's population, and Asian countries accounted for more than one-half of the 136 million children born during the year 2000 [*Population Reference Bureau*, 2000, available at http://www.prb.org/asia_near_east/asia_background.html]. This increasing population, and its accompanying industrialization, is expected to produce an increase in pollution. The long-range transport of pollutants from all locations, including the Asian continent, is a topic of current interest that needs to be better understood.

[3] Meteorological conditions during northern hemispheric springtime maximize the eastward transport of Asian air parcels. These parcels may have entered Asia with emissions acquired farther upstream, i.e., from Europe or even North America. Transport across the Pacific is achieved through active convection over the Asian continent and by seasonally strong westerly winds [*Merrill*, 1989]. Typical flow patterns for spring are shown in Figure 1. Northern hemispheric 300-hPa streamlines (Figure 1a) are dominated by flow from the west. However, the anticyclone east of the Philippines (15°N, 132°E) and its mirror image in the Southern Hemisphere produce easterly flow over the equator west of 160°E. The jet stream is strongest near Japan (not shown), and its speeds in excess of 70 m s^{-1} can yield transit times between Asia and North America of only a few days. In the lower troposphere, the streamlines at 1000 hPa (Figure 1b) show a major anticyclone (30°N, 153°W) dominating the northern Pacific. Strong subsidence associated with this anticyclone occurs over the subtropical northeastern Pacific (not shown). The Southern Hemisphere anticyclone is located west of South America (30°S, 100°W). Outflow from the two anticyclones forms the northeasterly and southeasterly trade winds that merge at the intertropical convergence zone (ITCZ).

[4] Several studies have examined the springtime transport of Asian pollutants over the North Pacific. *Kaneyasu et al.* [2000] considered the outflow from coastal Asia to be a "gate" to the North Pacific through which cold, highly polluted air is transported northeastward. Based on a one-year climatology of atmospheric transport, *Stohl* [2001] found that midlatitude cyclones carried pollution away from the Asian continent, with some air reaching Alaska and the western coast of the contiguous United States. *Jaffe et al.* [1999] also noted that Asian anthropogenic emissions significantly impacted the concentrations of many atmospheric species arriving over North America during spring. Similarly, both *Bernsten et al.* [1999] and *Jacob et al.* [1999] used three-dimensional chemical transport models to study the impact of Asian emissions on concentrations of pollutants over the United States. *Talbot et al.* [1997] described significant Asian outflow in the western Pacific Basin

[1]Department of Meteorology, Florida State University, Tallahassee, Florida, USA.
[2]University of California, Irvine, California, USA.
[3]NASA Langley Research Center, Hampton, Virginia, USA.
[4]Harvard University, Cambridge, Massachusetts, USA.

0148-0227/02/2001JD001418

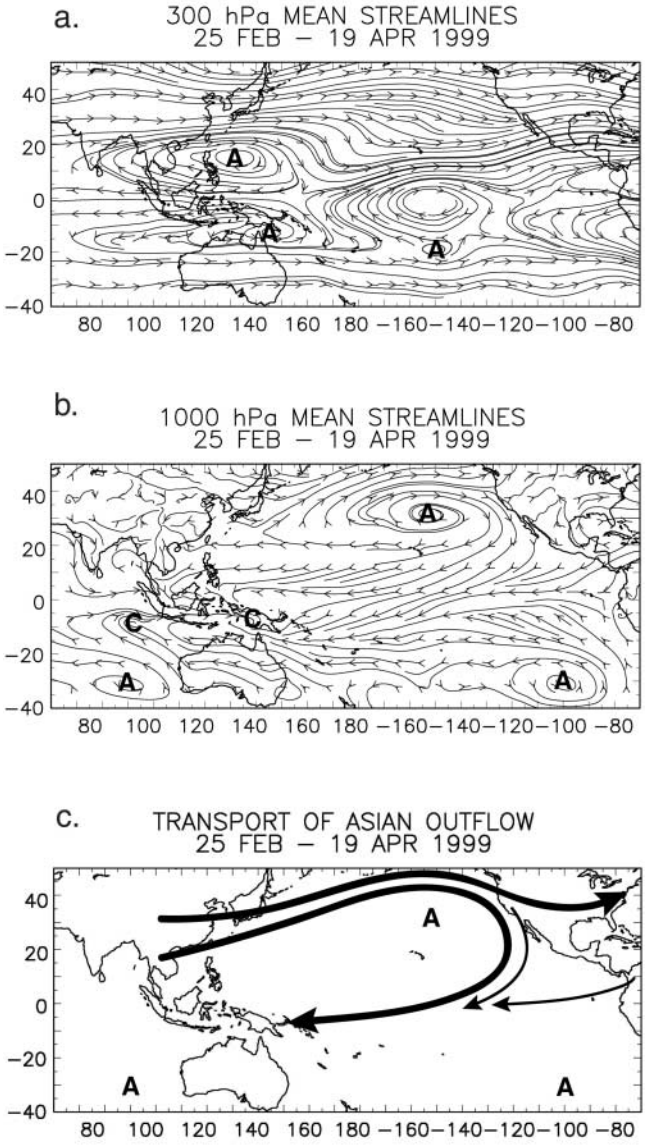

Figure 1. Mean streamlines during the PEM T-B period (25 February–19 April 1999) for a) 300 and b) 1000 hPa. Anticyclonic centers are denoted "A," while cyclonic centers are denoted "C" [after *Fuelberg et al.*, 2001]. c) Schematic of Asian outflow and "tributaries" from the Americas. Anticyclonic centers at 1000 hPa have been superimposed for reference.

during NASA's PEM West-B experiment, with industrial pollutants transported eastward at both lower and upper levels by convective and synoptic scale flows. By comparing transport during PEM West-B with that during the earlier PEM West-A mission, *Gregory et al.* [1997] concluded that greater Asian outflow occurred during northern hemispheric spring than summer. They also found that Asian sources dominated the northern hemispheric continental influence on pristine areas of the Pacific.

[5] NASA's Pacific Exploratory Mission to the Tropics Phase-B (PEM T-B) was conducted during northern hemispheric late winter and early spring (25 February–19 April 1999) [*Raper et al.*, 2001]. The mission provided a seasonal contrast with the PEM T-A mission (14 August–6 October 1996). Several investigators have examined chemical transport during PEM T-B. *Blake et al.* [2001] observed enhanced concentrations of trace gases such as Halon-1211 and methyl chloride (CH_3Cl), species that are attributed to Chinese Halon gas production and Asian biomass burning plumes, respectively. *Clarke et al.* [2001] described the sampling of Asian pollution 10,000 km away from its source. Their investigation confirmed that a "river-like" transport of Asian dust and pollution could be maintained over very long distances. In addition, *Maloney et al.* [2001] found that backward trajectories and corresponding chemical measurements sometimes revealed long-range transport from Asia that extended into the tropics. Logan et al. (unpublished manuscript) has described coherent layers of enhanced CO and hydrocarbons over the North Pacific, primarily north of 15°N. Enhanced layers in the marine boundary layer gave no indication of biomass burning, and their backward trajectories tracked over the North Pacific, crossing the Asian continent north of 35°N. Conversely, layers above 3 km exhibited enhancement ratios that were more similar to those of biomass burning. Their trajectories crossed the Pacific further south than those of the lower altitude group.

[6] This paper investigates a specific type of long-range transport during the PEM T-B period that to our knowledge has not been documented rigorously. Figure 1c shows the specific transport pathway on which we focus. First, upper tropospheric westerly winds in the middle latitudes transport parcels from Asia (and locations farther upstream) eastward across the Pacific. Parcels in the northern part of this flow regime continue rapidly eastward toward North America; however, the more southern parcels encounter subsidence and curve southward due to the semipermanent subtropical anticyclone. These parcels may receive fresh injections of pollution from North or Central America. Finally, parcels that continue south are transported westward by the trade winds and are carried to the western tropical Pacific. Thus, we hypothesize that some Asian outflow follows a long looping pattern over a period of several weeks, ultimately extending to near Indonesia. To investigate this hypothesis, four flights during the PEM T-B mission have been selected for detailed meteorological and chemical examination. We will describe the mechanisms responsible for the transport and subsequent chemical aging and dilution experienced by Asian sourced air masses.

[7] We will denote this transport pathway a "river of pollution," a term frequently used by the PEM T-B Science Team. However, readers should note that the term is merely a metaphor used to assist in describing the current transport processes. A river over land starts out as a small creek and becomes larger by collecting more water along the way. However, the air in our "river of pollution" experiences entrainment after leaving its source regions, and this decreases the concentration of pollutants. Information about the episodic character of our "river" is given later in the text.

2. Data and Methodology

2.1. Meteorological Data

[8] NASA's DC-8 and P-3B aircraft collected chemical data over the tropical Pacific during the PEM T-B mission

[*Raper et al.*, 2001]. We used meteorological data from the *European Centre for Medium-Range Weather Forecasts* (*ECMWF*) [1995] to describe conditions during the flights. The gridded global ECMWF data were at $1° \times 1°$ latitude/longitude horizontal resolution, with 51-sigma levels in the vertical. They were available at 0000, 0600, 1200, and 1800 UTC. To facilitate the calculations, the computational domain was reduced to 30°S–70°N and 105°E eastward to 95°W. The lowest 30-sigma levels were interpolated to 20 constant pressure levels between 100 and 1013 hPa.

[9] Backward trajectories were calculated using the kinematic method that utilizes the three dimensional wind components. The kinematic method has been widely used in previous studies [e.g., *Maloney et al.*, 2001; *Fuelberg et al.*, 1999, 2000, 2001; *Hannan et al.*, 2000; *Stohl and Trickl.*, 1999; *Garstang et al.*, 1996; *Krishnamurti et al.*, 1993]. Details about our trajectory model, including a comparison between kinematic and isentropic trajectories, are found in the studies by *Fuelberg et al.* [1996, 1999, 2000]. One difference from these earlier applications is that current trajectories were not terminated if they reached the model's lower boundary. Instead, we permitted them to continue isobarically until upward vertical motion carried them to higher altitudes. This procedure is similar to that used by *Stohl et al.* [1995]. Trajectories intersecting terrain above the lower model boundary ended at that location.

[10] Our backward trajectories arrived along horizontal portions of the DC-8 and P3-B flight tracks at 5-minute intervals of flight time. At a typical aircraft ground speed of 300 kt ($\sim$150 m s^{-1}), this interval corresponds to a horizontal separation of 45 km. Arrival locations during aircraft ascents and descents were at a 50-hPa interval. Horizontal and vertical wind shear cause trajectories to disperse, producing an uncertain origin for the region in question. Calculating trajectories in clusters helps reveal locations where this uncertainly is likely [e.g., *Merrill et al.*, 1985; *Kahl*, 1993]. Therefore, we calculated trajectories on a 15-point diamond cluster centered on each 5 min location along the flight track. Points of the diamond were spaced 2° latitude/longitude from the center location (5 points). The pattern was repeated above and below (at ±25 hPa) to complete the cluster (10 additional points). At locations where the +25 hPa separation placed cluster points below the model boundary, the 1013 hPa level was substituted. The six hourly ECMWF data closest to the flight time were used as the arrival time for that flight's trajectories, i.e., 0000 UTC was used in the four cases examined here.

[11] Trajectories are subject to various uncertainties due to the numerics of the trajectory model, the spatial and temporal resolution of the ECMWF data, errors in the placement of meteorological features, and the sparseness of input data, e.g., *Stohl et al.* [1995], *Stohl and Seibert* [1998], and *Doty and Perkey* [1993]. Since the Pacific Basin is a relatively data sparse region, meteorological features will be depicted less accurately than in more data-rich regions. In addition, the horizontal and temporal resolution of the ECMWF data means that subgrid scale processes such as boundary layer mixing and deep convection cannot be accurately resolved. Thus, convective scale transport due to individual updrafts and downdrafts is not depicted, and as a result, the associated trajectories do not represent these smaller scale transport mechanisms. The combination of each of the factors listed above leads to trajectories whose uncertainty increases with time.

2.2. Chemical Data

[12] An extensive set of in situ chemical data was collected during the PEM T-B campaign. Sampling intervals varied from 1 to 1200 s depending on the analytical method being used. *Raper et al.* [2001] discuss the various species that were measured, including the techniques used to make the measurements, their temporal resolution, and the limit of detection (LOD) for each instrument. A series of merged data sets was created by the atmospheric chemistry group at Harvard University. These merged data sets placed flight information and various chemical measurements on a common time interval. Since many species that we examine here were collected using whole air sampling, we have employed the data merge in which the higher frequency data were averaged over the whole air sample periods. These sampling times ranged in duration from of 8 to 80 s depending on aircraft altitude. Further details about whole air sampling procedures, including variations in the temporal resolution, analytical accuracy, and precision can be found in the work of *Blake et al.* [2001]. This merged chemical data set linked our trajectories to the chemical tracer measurements made along the flight tracks.

[13] Various chemical species can be used to infer the origin and possible lifetime of an air sample [e.g., *Mauzerall et al.*, 1998; *Blake et al.*, 2001; *Blake et al.*, 1996; *Maloney et al.*, 2001]. The characteristics of species used in the current study are described below.

[14] Photochemical lifetimes relevant to the PEM Tropics B observations were estimated for CO and the other tracer species along the transport paths investigated in this study. Since rates of photochemical processing vary with latitude and altitude, separate lifetimes were calculated for representative midlatitude and equatorial transport paths. Equatorial lifetimes were based on OH estimates calculated from in situ observations. These observations adequately spanned the equatorial transport path in Figure 1c. However, due to a lack of in situ data, lifetime estimates for transport over the North Pacific were based on calculations along back trajectories generated for this study. Calculations were performed using a model previously described by *Crawford et al.* [2000]. These calculations did not consider dilution, but did account for changes in the ozone column along hypothetical trajectories. Values of ozone, CO, water vapor, and temperature were held constant. Due to the sensitivity of OH to concentrations of NO_x, calculations were made for two scenarios. A calculation holding NO_x constant was done under the assumption that the observed NO_x was sustained along the trajectory by reservoir species (e.g., PAN and HNO_3). This assumption leads to a conservative OH estimate. A second calculation was done by invoking an initial value for NO_x that is large enough to explain the observed NO_x at the end of the trajectory through photochemical decay. This assumption is associated with the other extreme, resulting in a greater OH estimate.

[15] Lifetime estimates were based on calculated, diurnally averaged values for OH along these transport paths. For cross-Pacific, middle latitude transport between Asia and

Table 1. Estimated Photochemical Lifetimes of Chemical Tracers for Conditions Observed During PEM T-B

Species	Midlatitude Lifetime, Middle Troposphere	Midlatitude Lifetime, Lower Troposphere	Equatorial Lifetime, Boundary Layer
CO	3.4–5.1 months	2.2–3.0 months	1.1–2.4 months
Ethene (C_2H_4)	2.4–3.6 days	1.9–2.6 days	0.9–2.0 days
Propane (C_3H_8)	26–40 days	17–23 days	7–16 days
Ethyne (C_2H_2)	35–55 days	24–32 days	11–23 days
Ethane (C_2H_6)	5.1–7.7 months	2.8–3.8 months	1.1–2.4 months
Perchloroethylene (C_2Cl_4)	8.0–12.0 months	4.1–5.6 months	1.8–2.8 months
Methyl chloride (CH_3Cl)	3.5–5.19 years	1.6–2.2 years	0.6–1.3 years
Halon-1211	357–535 years	282–384 years	142–306 years

the West Coast of the United States in the middle troposphere (see Figure 1c), diurnally averaged OH was estimated at 4 to 6 $\times$ 10^5 molecules cm^{-3}. Slightly greater OH of 5.5 to 7.5 $\times$ 10^5 molecules cm^{-3} was estimated for midlatitude transport in the lower troposphere. For westward cross-Pacific transport at equatorial latitudes in the lower troposphere (see Figure 1c), estimates for diurnally averaged OH were in the range of 7 to 12 $\times$ 10^5 molecules cm^{-3}.

[16] Calculated lifetimes of the species that were investigated are given in Table 1. For the reference species CO, lifetimes range from several months at midlatitudes to as short as one month in the tropics. Ethene (C_2H_4) is a by-product of combustion, and it has been suggested that it also is emitted by the ocean [*Riemer et al.*, 2000]. Its lifetime is the shortest; only several days at midlatitudes, diminishing to less than 2 days in the tropics. Propane (C_3H_8) and ethane (C_2H_6) are emitted during petroleum refining and natural gas distribution. Propane also is a fuel source for cooking and heating [*Blake and Rowland*, 1995], with a typical midlatitude lifetime of $\sim$1 month, but only 1–2 weeks in tropical regions. Ethyne (C_2H_2) is a useful tracer of incomplete combustion from both fossil fuel and biomass burning [*Blake et al.*, 1999]. The lifetime of ethyne is slightly longer than that of propane, while ethane has a significantly longer lifetime more similar to that of CO. Perchloroethylene (C_2Cl_4) is an industrial solvent that often is used as an industrial tracer [e.g., *Gregory et al.*, 1997; *Blake et al.*, 2001]. Its typical atmospheric lifetime ranges from several months to a year, although its lifetime in the tropics is comparable to that of ethane and CO. Methyl chloride (CH_3Cl) is an indicator of biomass combustion [*Rasmussen et al.*, 1980] with a lifetime up to several years at midlatitudes. Finally, the fire retardant Halon-1211 [*Montzka et al.*, 1999] has a lifetime exceeding one hundred years. Due to its high ozone destruction potential, production of Halon-1211 has ceased in developed countries such as the United States, Japan, and those in Europe. As of 1999, China was the sole producer of Halon-1211 [*United Nations Environment Programme* (*UNEP*), 1991; *UNEP, Nairobi, Kenya*, 1999, available at http://www.teap.org]. Emissions of Halon-1211 are strongly associated with the Asian continent [*Fraser et al.*, 1999].

[17] In general, dilution is expected to play the dominant role in the trends for these species along the transport paths highlighted in Figure 1c, especially for the longer lived species. Nevertheless, photochemistry also will make varying contributions to the trends in these species given the expected transport times of 20–25 days from Asia eastward and then westward across the tropical Pacific. Based on the lifetimes in Table 1, only CH_3Cl and Halon-1211 can be considered inert over this path.

3. Results

[18] Our objective is to document the hypothesized "river of pollution" that leaves the coast of Asia, flows eastward in the middle troposphere, and later turns to the west in the lower altitudes (Figure 1c). We examined all of the PEM T-B flights, and the two P-3B and two DC-8 flights that best illustrate this transport path are shown in Figure 2. The results will show that these four flights represent a northeast to southwest sampling of the "river" at different downstream locations. It should be emphasized that the chemical and trajectory data for the four selected flights do not represent a Lagrangian sampling of the "river." Instead, the "river" or "current" is sampled at various locations along its length. Day-to-day atmospheric variability can change the transport paths of emissions from the same source. This varying transport coupled with photochemical processes will affect the mixing ratios of chemical species with increasing distance from their source [*McKeen et al.*, 1996].

3.1. P-3B Flight 4, Dryden to Hilo

[19] P-3B Flight 4 (Figure 2) was a transit flight that headed west-southwest from NASA's Dryden Research Facility, California (34.9°N, 117.9°W) to Hilo, Hawaii (19.7°N, 155.0°W) on 11 March 1999. Time series of aircraft altitude and selected chemical data from 2000 UTC 11 March to 0100 UTC 12 March are plotted in Figure 3. After takeoff at 1933 UTC, the P-3B ascends to flight level at $\sim$550 hPa ($\sim$4.8 km). Shortly thereafter (at 2005 UTC), a major change in chemical composition begins and lasts through 2036 UTC. CO increases from a background mixing ratio of $\sim$80 ppbv to a maximum of 248 ppbv. In addition to the enhanced CO, values of CH_3Cl, Halon-1211, ethyne (C_2H_2), and ethene (C_2H_4) spike in a similar manner. Based on the work of *Mauzerall et al.* [1998], we will define a "plume" using the criterion that the sampled air must exhibit CO values that are enhanced at least 20 ppbv above the local background. The plume will consist of the entire period of enhancement, extending from the preceding minimum to subsequent minimum. We will denote this first period of enhanced CO (2005 UTC to 2036 UTC) as "Plume 1."

[20] When the P-3B begins to descend to the marine boundary layer, a second change in chemical characteristics occurs, lasting from 2037 to 2157 UTC. Compared to

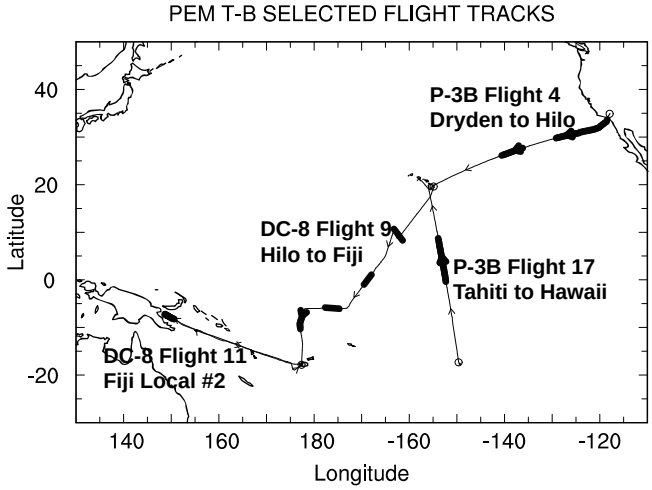

Figure 2. Flight tracks of the two P-3B and the two DC-8 missions examined in this study. Bold portions along the flight tracks indicate locations of the plumes being examined.

Plume 1, the CO value of ~150 ppbv is somewhat smaller but still enhanced compared to values before and after. The CO signature remains nearly constant during the period. The biomass burning (CH_3Cl) and Asian (Halon-1211) tracers decrease to some of the smallest values of the entire flight. The two industrial tracers C_2Cl_4 and propane (C_3H_8), as well as ethene (C_2H_4) and ethyne (C_2H_2), remain enhanced throughout the low level run. We will define this period of enhanced CO as "Plume 2."

[21] A second boundary layer run begins after 2300 UTC (Figure 3). The chemical signature of this region generally is similar to that of Plume 2; however, most current values are somewhat smaller. For example, the CO value is ~130 ppbv, not the ~150 ppbv of Plume 2. Although the two industrial tracers C_2Cl_4 and propane (C_3H_8), as well as ethyne (C_2H_2) are reduced from the previous low level run, they still are clearly enhanced relative to the values at higher altitudes. However, values of ethene (C_2H_4) remain small during the period, showing little difference with those from outside the interval. This third period of enhanced CO will be denoted "Plume 3." We next present trajectory analyses to determine the sources of the three chemical plumes.

[22] Ten-day backward trajectories from Plume 1 are shown in Figure 4a. The top panel shows a horizontal perspective of the clusters, while the lower panel is a plot of pressure altitude versus longitude. Small arrows along the trajectory paths indicate locations at one-day intervals, while large arrows denote locations at five-day intervals (as well as 10-day intervals for the 15-day trajectories shown later). An "x" at the end of a trajectory indicates that the parcel has exited the computational domain before completing the 10-day period. Conversely, an asterisk "*" indicates that the trajectory has completed the 10-day period within the data domain.

[23] The clusters of trajectories corresponding to Plume 1 (Figure 4a) arrive at the P-3B after rapid transport across the Pacific. Many of the trajectories extend to the western edge of the data boundary in as few as five days. Some travel over southern China at relatively high altitudes and may not be influenced greatly by surfaced-based sources. However, other trajectories travel near the surface and then ascend and merge with those from further west. Imagery from the Japanese Meteorological Agency's GMS-5 satellite (not shown) suggests that vertical motions associated with the warm conveyer belt of a nearby wave cyclone are responsible for the ascent of these near surface parcels. This combination of parcels then is carried the length of the Pacific in ~3.5 days. Their paths over the Pacific comprise a coherent "bundle," suggesting relatively little mixing with the surroundings [e.g., *Stohl*, 2001; *Wernli and Davies*, 1997]. As they approach North America, they are influenced by a ridge associated with the subtropical anticyclone (as in Figure 1) where they turn southeastward and descend to their P3-B arrival altitudes near 550 hPa.

[24] The ~3.5 day transit time across the Pacific (Figure 4a) is short enough that values of ethene (C_2H_4), whose typical lifetime ranges from 2.4 to 3.6 days (Table 1), can remain enhanced far removed from an Asian source. The close proximity of some trajectories to the west coast of North America suggests that Plume 1 could be influenced by this nearby continental source (Figure 4a). However, radiosonde data along coastal California as well as in-flight

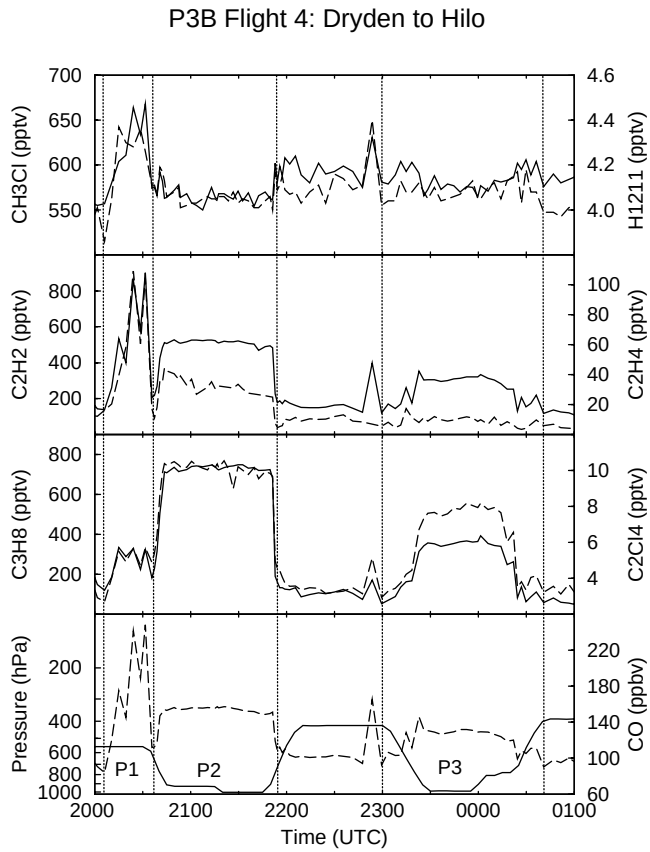

Figure 3. Time series of CH_3Cl (pptv), Halon-1211 (pptv), C_2H_2 (pptv), C_2H_4 (pptv), C_3H_8 (pptv), C_2Cl_4 (pptv), aircraft altitude (hPa), and CO (ppbv) along a portion of P-3B Flight 4. Values corresponding to the left ordinate axes are plotted with a solid line; a dashed line corresponds to values on the right ordinate axes. Plumes lie between the dotted vertical lines (Plumes 1, 2, and 3 (P1–P3), respectively).

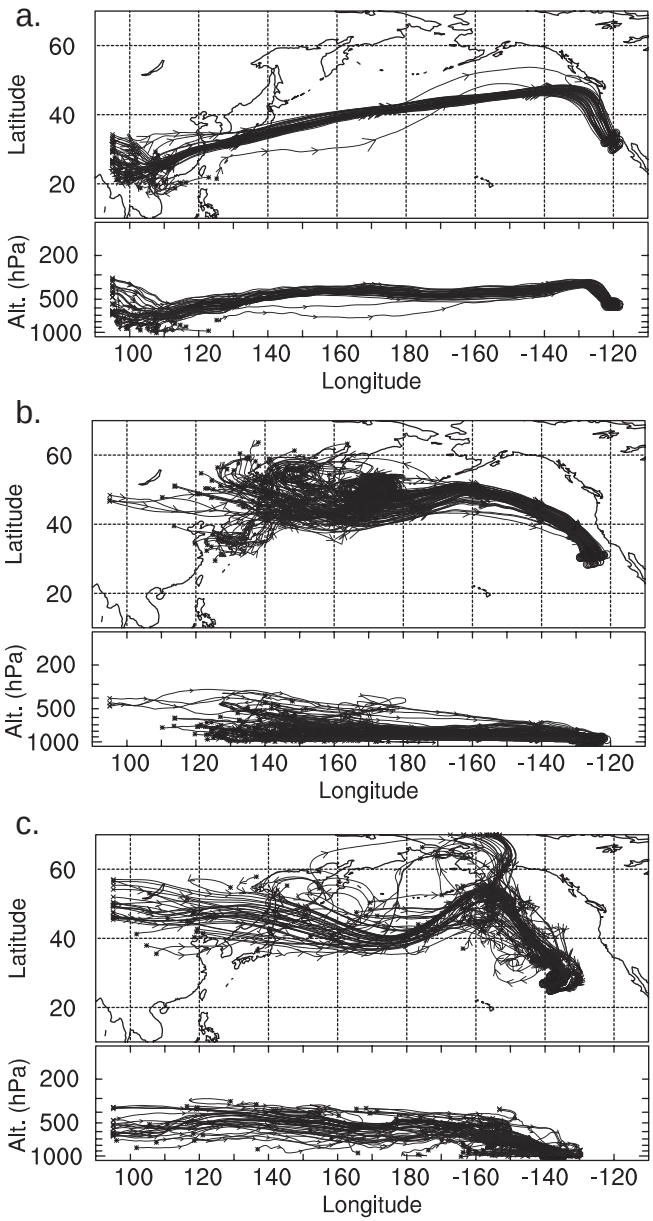

Figure 4. Clusters of 10-day backward trajectories arriving at the three plumes of P-3B Flight 4, a) Plume 1, b) Plume 2, and c) Plume 3. Circles indicate arrival locations; arrows denote trajectory locations at daily intervals. The upper panel of each group is a plan view; the lower panel is longitude versus altitude (hPa). The trajectories arrive at 0000 UTC 12 March 1999.

measurements of temperature and dew point show a strong capping subsidence inversion in the area due to the high pressure. Thus, continental pollution from this source will tend to be confined to the atmospheric boundary layer. Nonetheless, *Angevine et al.* [1996] note that pollutants can be advected over or under capping inversions by sea breezes and other mesoscale phenomena that are not resolved the ECMWF data. *Simpson* [1994] provides an extensive description of the structure of sea breezes and the circulations that are associated with them.

[25] To better determine characteristics of Plume 1, we performed a linear least squares regression for each of the previously mentioned trace gases relative to CO. Our procedures are similar to those used by *Blake et al.* [2001] and *Mauzerall et al.* [1998]. The slope of the regression provides the plume's enhancement ratio relative to the local background, giving information about its possible age and source. For example, plumes from urban sources have well correlated regressions between the industrial tracers and CO [*Blake et al.*, 1999]. Similarly, plumes with highly correlated values of CH_3Cl to CO indicate a biomass burning source. A mix of biomass and industrial sources is indicated by both types of tracers being highly correlated with CO.

[26] Figure 5 shows the correlations for Plume 1. The biomass burning tracer CH_3Cl, as well as ethyne (C_2H_2) and ethene (C_2H_4), exhibit highly correlated regressions, with r^2 values greater than 0.90. The strong correlation ($r^2 = 0.93$) for the short-lived species ethene (C_2H_4) suggests that Plume 1 is only a few days removed from its source, as suggested also by the trajectories (Figure 4a). There are moderate correlations for both Halon-1211 ($r^2 = 0.61$) and propane (C_3H_8) ($r^2 = 0.71$). On the other hand, the industrial tracer C_2Cl_4 is poorly correlated with CO ($r^2 = 0.34$). Both propane (C_3H_8) and C_2Cl_4 exhibit relatively small slopes. The lack of C_2Cl_4 enhancement indicates that urban/industrial pollutants do not contribute significantly to this plume.

[27] The trajectory data indicate that southeastern Asia is the most recent source region for Plume 1 (Figure 4a). And, this meteorological based finding is consistent with the chemical data within the plume, especially the strong biomass burning signature seen in the enhancement ratio of CH_3Cl to CO (Figure 5). Global fire data for March 1999 from the Along Track Scanning Radiometer (ATSR) show that regions of southern Asia contain a large number of fires (Figure 6). These areas correspond to both origination points and overpass locations for the Plume 1 trajectories. The enhanced Halon-1211 signature also suggests that Plume 1 has an Asian origin.

[28] It is informative to consider future locations of parcels comprising Plume 1. Figure 7 contains 10-day forward trajectories calculated from Plume 1's location along the P-3B flight track (i.e., the arrival points east of 120°W). These relatively high altitude/high latitude forward trajectories initially move southward near Baja California, but then abruptly recurve toward North America due to a reversal in winds associated with a low pressure trough. Thus, the parcels do not head southwestward to form the "river of pollution."

[29] We next examine Plume 2 in greater detail. Backward trajectories from Plume 2 (Figure 4b) exhibit a less coherent pattern than those of Plume 1 (Figure 4a). Parcels are transported from a broad area of northeastern Asia and Japan, and then pass through a series of midlatitude wave cyclones (the looping patterns in Figure 4b) as they progress eastward. Unlike Plume 1's trajectories, the current trajectories do not extend over areas of southern China where biomass burning is prevalent (Figure 6). Most of Plume 2's trajectories remain in the mid to low troposphere throughout their 10-day transits. However, midway through their eastward paths, many are influenced by subsidence associated with the subtropical anticyclone centered north of Hawaii,

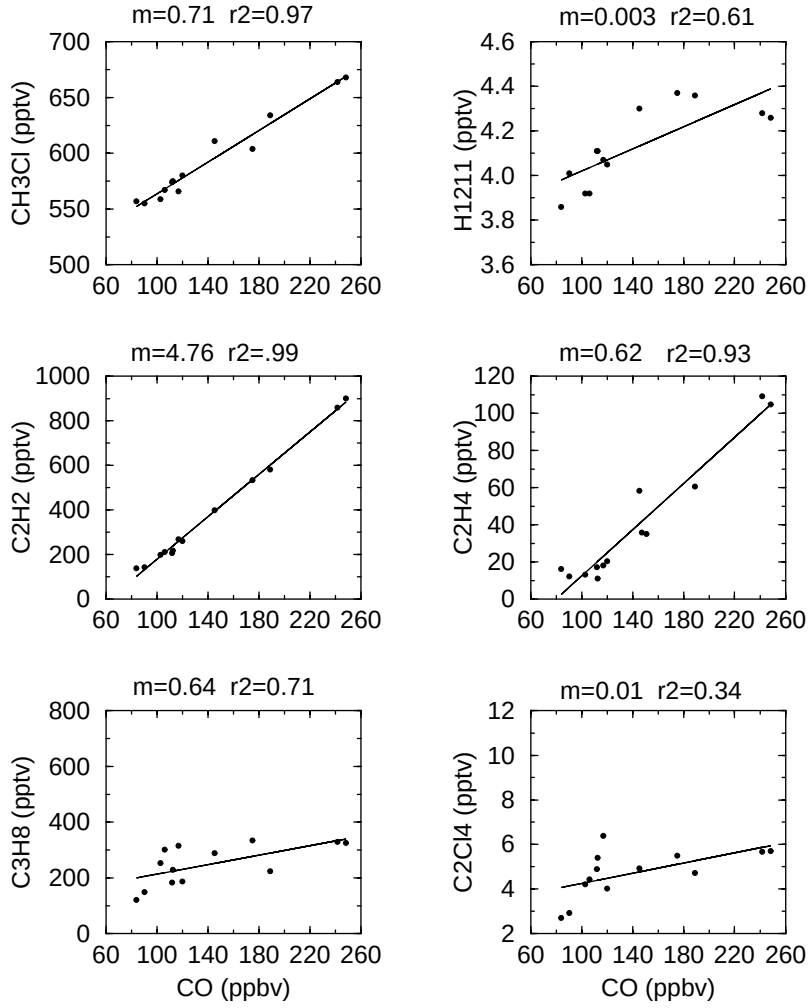

Figure 5. Correlation plots for Plume 1 of P-3B Flight 4 for CH_3Cl (pptv), Halon-1211 (pptv), C_2H_2 (pptv), C_2H_4 (pptv), C_3H_8 (pptv), and C_2Cl_4 (pptv) versus CO (ppbv). Linear regressions are shown for each correlation. The slopes (m) of the regressions represent the enhancement ratios.

causing them to descend further. Northwesterly flow then transports the parcels southeast toward the P-3B flight track.

[30] Correlation plots for Plume 2 (not shown) are not informative since values of most species are very uniform during the period. However, the strongly enhanced values of C_2Cl_4 and propane (C_3H_8), for example (Figure 3), together with the small values of CH_3Cl are consistent with industrial sources in northern Asia and Japan. The recently completed TRACE-P mission (February–April 2001) sampled a "Shanghai plume" over the Yellow Sea that had an "initial" ethene (C_2H_4) to CO ratio of ~2 pptv/ppbv (i.e., 2440 pptv of ethene (C_2H_4) for 1200 ppbv of CO) (D. Blake, personal communication). In contrast, Plume 2 of P-3B Flight 4 has peak values of ~40 pptv of ethene (C_2H_4) to ~150 ppbv CO. Based on ethene's middle latitude lifetime being <4 days (Table 1), we believe that a diminished amount of this tracer would remain after a 7 to 10 day transit from Asia. Alternatively, although the trajectories in Figure 4b do not indicate low level outflow from North America, mesoscale processes such as land/sea breezes or topographic circulations [e.g., *Angevine et al.*, 1996] not resolved by the ECMWF data could transport ethene from coastal California, providing a fresh source injection. This possibility is described by *Blake et al.* [2001].

[31] Plume 2 is located farther south than Plume 1 and is at a lower altitude, probably having experienced greater subsidence associated with the subtropical anticyclone. Forward trajectories originating from Plume 2 (Figure 7) travel south and then southwest in response to the northeasterly trade winds. These forward trajectories, together with the backward trajectories seen earlier (Figure 4b), indicate that parcels can reach equatorial regions between 10 and 15 days after leaving Asia. This pathway is consistent with the river of pollution shown in Figure 1c.

[32] Ten-day backward trajectories from the second boundary layer run (i.e., Plume 3, Figure 4c) mostly originate over northeastern Asia. However, if extended beyond ten days, many likely would have passed over Europe and even North America. Since the ten-day trajectories begin in the middle troposphere (~500 hPa) where wind speeds are relatively strong, they initially travel eastward quite rapidly. However, during the final five days they descend to altitudes having much slower speeds. Compared to Plume 2's trajectories, the Plume 3 trajectories spend ~3 additional

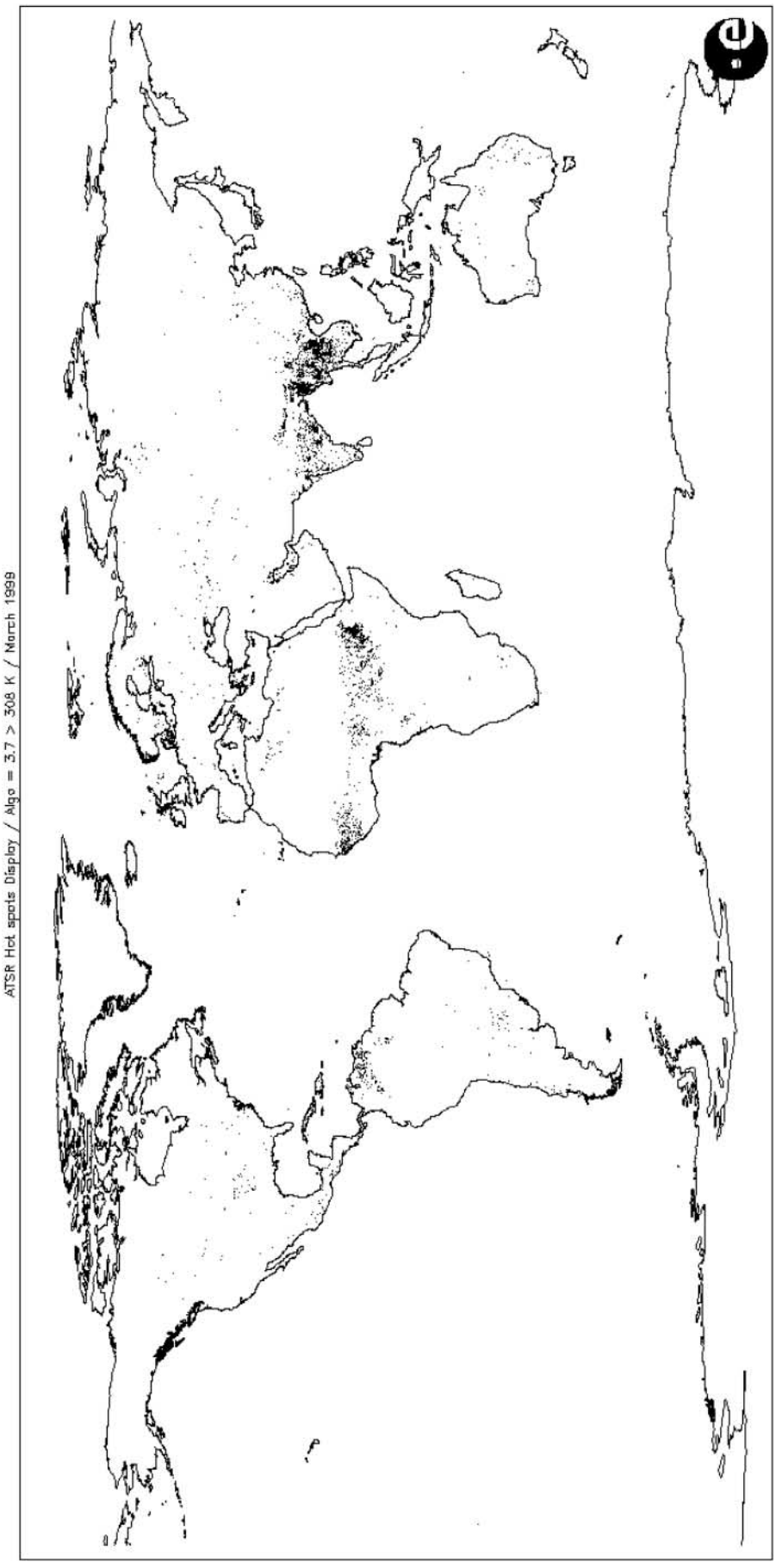

Figure 6. Along Track Scanning Radiometer (ATSR) global fire map for March 1999. Black dots indicate fire locations. Data were available through the Internet (http://shark1.esrin.esa.it).

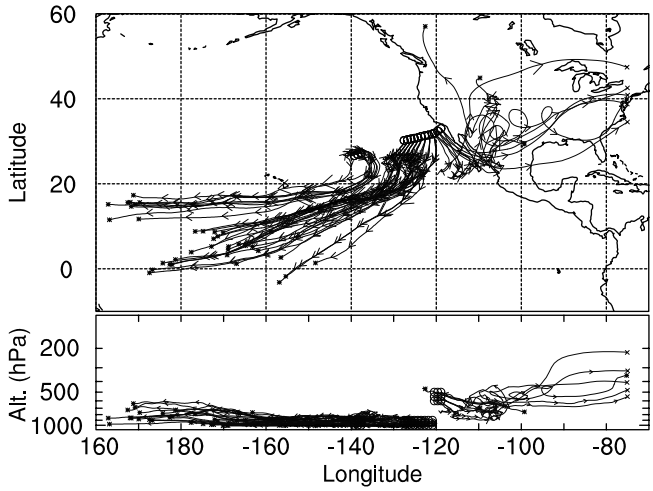

Figure 7. Ten-day forward trajectories originating from Plumes 1, 2, and 3 of P-3B Flight 4. The origination time is 0000 UTC 12 March 1999 and the ending time is 0000 UTC 22 March 1999.

days in the tropical latitudes. Thus, they experience relatively warm tropical conditions and greater solar zenith angles for a longer time. We believe these factors contribute to the diminished chemical signature that is apparent in Figure 3. Ten-day forward trajectories from Plume 3 (Figure 7) head west-southwest toward the tropics, remaining somewhat north of those from Plume 2. This path probably is near the northern extent of the low-level river of pollution.

[33] To summarize the results of P-3B Flight 4, the three plumes primarily represent the eastward transport of Asian outflow (and even older upwind emissions) across the Pacific Ocean. The higher latitude Plume 1 parcels remained in the upper levels and were rapidly transported eastward to the P-3B sampling site by strong westerly winds. They ultimately reached North America. Conversely, the lower latitude Plume 2 and 3 parcels had descended into the lower troposphere while crossing the Pacific. They subsequently turned southwestward and headed toward the tropics. The following sections describe transport mechanisms and in situ chemical data during flights over downstream regions of the "river."

3.2. P-3B Flight 17, Tahiti to Hawaii

[34] P-3B Flight 17 (Figure 2) was a transit flight that departed Tahiti (17.5°S, 149.6°W) at 1900 UTC 9 April 1999 and headed north toward Honolulu, Hawaii (21.3°N, 157.9°W). Figure 8 shows the time series of aircraft altitude and chemical data between 2130 UTC 9 April and 2350 UTC 11 April that brackets the boundary layer sampling run just north of the equator. Since the short-lived species ethene (C_2H_4) is reduced to trace amounts (not shown), the longer-lived species ethane (C_2H_6) has been substituted in Figure 8 and in time series for later flights.

[35] Midway through its descent at 2200 UTC, the P-3B encounters an ~20 ppbv increase in CO above the local background. This relatively constant enhancement lasts until 2305 UTC, reaching a maximum of 79.5 ppbv, before decreasing to ~64 ppbv. Two brief episodes of enhanced CO reaching 80 ppbv occur at 2322 and 2335 UTC. CO then decreases to ~56 ppbv at 2355 UTC. Propane (C_3H_8), ethyne (C_2H_2), ethane (C_2H_6), C_2Cl_4, and CH_3Cl show similar enhancements and fluctuations during the period. Halon-1211 fluctuates somewhat above local background levels. This region of enhanced CO and other species represents the single boundary layer plume sampled during Flight 17. Although the signature indicates a combination of both anthropogenic and biomass burning sources, the mixing ratios of all chemical species are considerably smaller than those of Flight 4 (Figure 3).

[36] Due to the relatively slow northeasterly flow in the lower altitudes of the tropics, the backward trajectories for this and later flights have been extended to 15 days. Although trajectory uncertainty increases with longer duration, we are interested only in the major features of the transport that should still be reliable. The horizontal plot of trajectory clusters from the plume (Figure 9) exhibits three branches. The first is an equatorial/southern hemispheric branch whose 15-day origins range between 17°N and 25°S. With the exception of several trajectories passing over Nicaragua, this branch does not exhibit a continental source during the 15-day period. However, additional trajectories might reach Central or northern South America if the period

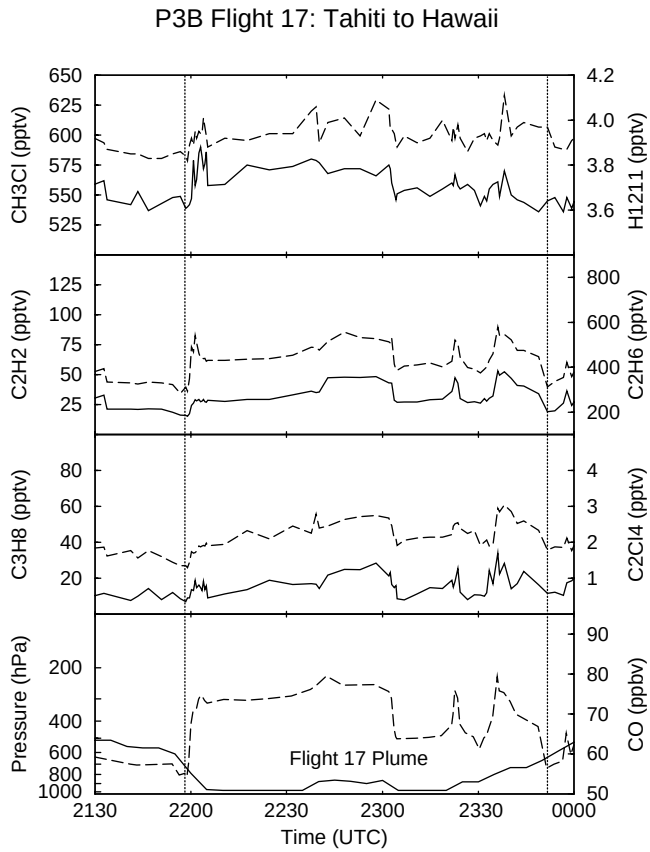

Figure 8. Time series of CH_3Cl (pptv), Halon-1211 (pptv), C_2H_2 (pptv), C_2H_6 (pptv), C_3H_8 (pptv), C_2Cl_4 (pptv), aircraft altitude (hPa), and CO (ppbv) along a portion of P-3B Flight 17. The single plume encountered on this flight lies between the dotted vertical lines. Values corresponding to the left ordinate axes are plotted with a solid line; a dashed line corresponds to values on the right ordinate axes.

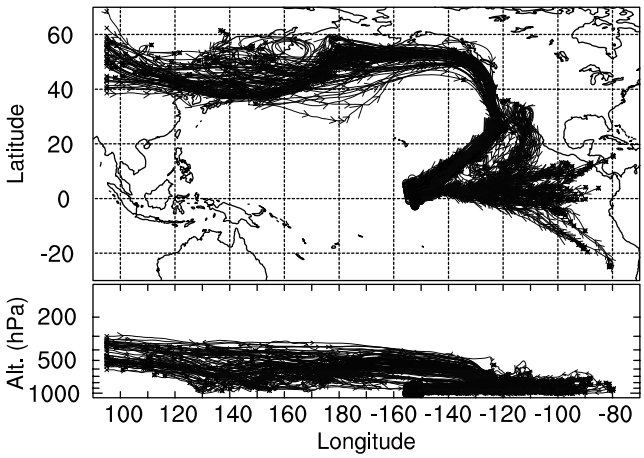

Figure 9. Clusters of 15-day backward trajectories arriving at the low-level plume of P-3B Flight 17. The trajectories arrive at 0000 UTC 10 April 1999.

were extended beyond 15 days. In addition, other trajectories might originate in the southern hemispheric middle latitudes in response to flow around the South Pacific anticyclone, i.e., the mirror image of the northern hemispheric pattern. A second group of trajectories has 15-day origins over the west coasts of the United States and northern Mexico. These parcels are transported southward by the anticyclonic flow, and once in the tropics, are carried southwestward by the trade winds. Altitudes of these two groups of trajectories change little. Both are most common along the southern end of the boundary layer run.

[37] A third group of trajectories (Figure 9) originates (at 15 days) over northeastern Asia and then passes over Japan at mid to upper levels before crossing the North Pacific. Their speeds are much greater than those of the other two groups, as evidenced by trajectories reaching the western data boundary in less than 15 days. They previously may have passed over Europe and North America. As observed with Plumes 2 and 3 of P-3B Flight 4 (Figure 4), these trajectories are influenced by the subtropical anticyclone over the North Pacific. Thus, they descend to lower altitudes along the California coast as they head south and then southwest toward the Flight 17 flight track.

[38] Since parts of Central America and equatorial South America produce urban source emissions [*Blake et al.*, 1999; *Talbot et al.*, 1996], the aged industrial signature of the Flight 17 plume (Figure 8) may represent a combination of North American, northern Asian, and equatorial/southern hemispheric sources (Figure 9). Concerning the biomass burning signature seen in CH_3Cl, a comparison of the March 1999 ATSR global fire map (Figure 6) and the backward trajectories indicates that the North American and northern Asian groups do not pass over areas of significant burning. However, burning is indicated in Central America and in South America (north of the equator). Thus, the biomass burning signature may originate from fires in these regions, with transit times greater than the 15 days period shown Figure 9.

[39] These additional pollution sources from the Americas can be considered "tributaries" of the main "river" that departs Asia (depicted in Figure 1c). We next examine regions even farther downstream of the "river," i.e., over the equatorial Pacific.

3.3. DC-8 Flight 9, Hilo to Fiji

[40] DC-8 Flight 9 (Figure 2) is the third PEM T-B mission that we use to document the "river of pollution." It was a cross equatorial transit flight from Hilo, Hawaii (19.7°N, 155.0°W) to Fiji (17.9°S, 176.9°E) that departed the Big Island at 2027 UTC 17 March 1999.

[41] The time series of chemical tracers and aircraft altitude (Figure 10) focuses on the four low-level sampling runs between 2300 UTC 17 March and 0600 UTC 18 March. During each of these descents into the marine boundary layer, CO is enhanced at least ~20 ppbv above the local background at higher altitudes. One should note that the enhanced values progressively decrease with each low level run as the flight heads southwest (from left to right in Figure 10). Greatest CO ranges from ~100 ppbv during the first run, to the smallest maximum of ~70 ppbv during the last run. These enhancements in CO will be denoted Plumes 1 through 4, respectively. One should note that our use of the term "plume" does not necessarily denote sharp tracer gradients, but also includes regions of somewhat

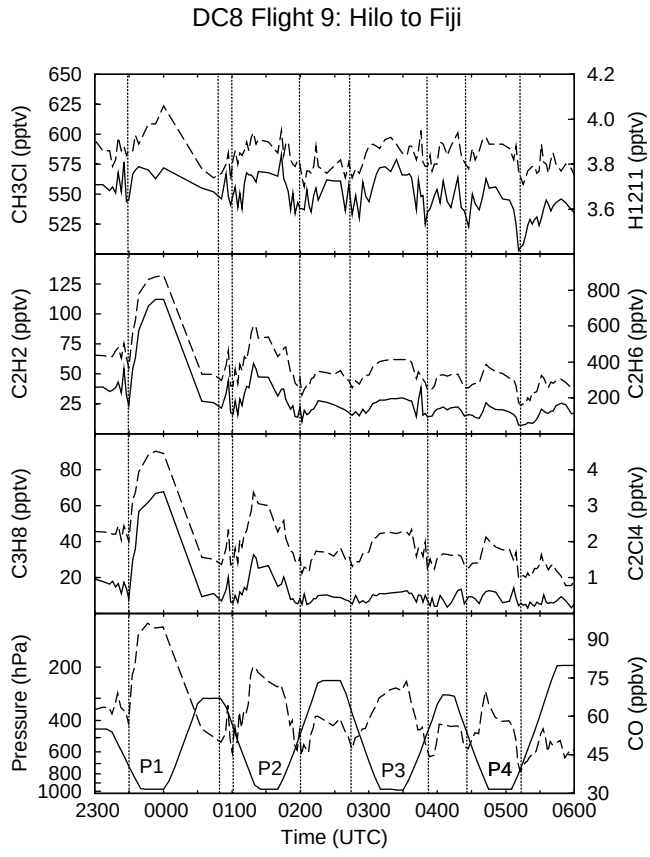

Figure 10. Time series of CH_3Cl (pptv), Halon-1211 (pptv), C_2H_2 (pptv), C_2H_6 (pptv), C_3H_8 (pptv), C_2Cl_4 (pptv), aircraft altitude (hPa), and CO (ppbv) along a portion of DC-8 Flight 9. Plumes lie between the dotted vertical lines (Plumes 1 through 4, respectively). Values corresponding to the left ordinate axes are plotted with a solid line; a dashed line corresponds to values on the right ordinate axes.

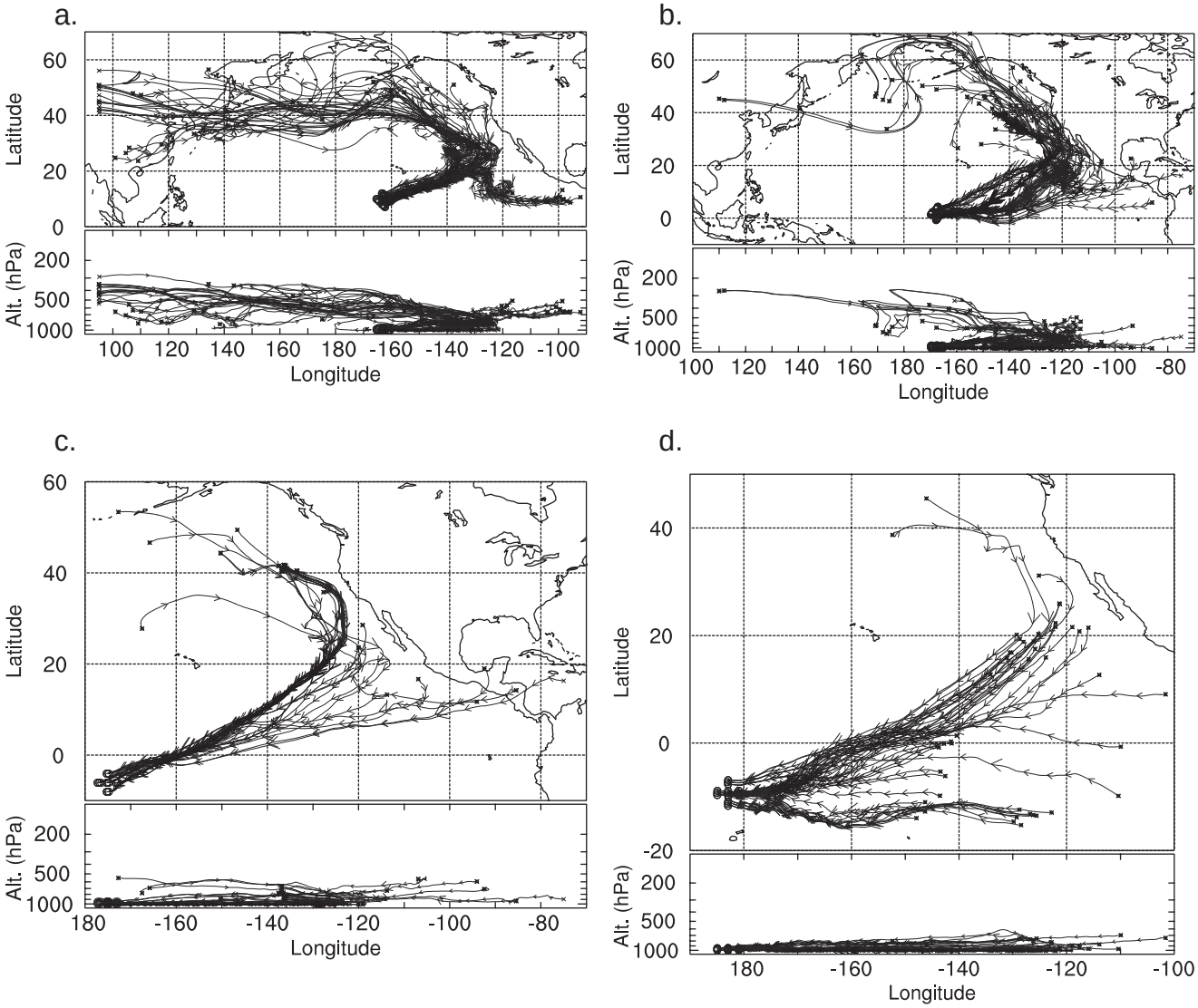

Figure 11. Clusters of 15-day backward trajectories arriving at the four plumes of DC-8 Flight 9, a) Plume 1, b) Plume 2, c) Plume 3, and d) Plume 4. The trajectories arrive at 0000 UTC 18 March 1999.

enhanced concentrations. Values of propane (C_3H_8) decrease steadily, becoming only slightly enhanced above the background (~10 pptv) during Plumes 3 and 4. Steady decreases also are observed in the industrial tracer C_2Cl_4 as well as ethyne (C_2H_2) and ethane (C_2H_6). Values of the biomass burning tracer CH_3Cl are greater in the lower levels than at higher altitudes, but they do not decrease with latitude as does CO. The Asian tracer Halon-1211 increases to 4.1 pptv in Plume 1 but remains at ~3.9 pptv for Plumes 2 through 4.

[42] The backward trajectories that follow indicate that Plumes 1–4 (Figure 10) are transported increasingly longer distances from their source regions over Asia and locations farther west. In addition, one should recall that the photochemical lifetimes of the various species become progressively shorter at lower latitudes (Table 1). The following paragraphs describe each of these plumes individually.

[43] Plume 1 was sampled during the first boundary layer run which extended from 2348 UTC 17 March to 0000 UTC 18 March. Its 15-day backward trajectories (Figure 11a) show predominant long-range transport off the Asian continent. The trajectories pass over highly industrialized Asian regions as well as southern Asia where biomass burning is occurring (Figure 6). A few trajectories probably originated over Central America. It is interesting that values of most chemical species in Plume 1 (Figure 10) are somewhat greater than those for the plume sampled during P-3B Flight 17 (Figure 8). The smaller values during Flight 17 may be due to the influence of southern hemispheric air (Figure 9) which is absent in the current case. This aspect will be discussed further in a later section.

[44] Plume 2 was sampled farther downstream, during the second boundary layer run between 0120 and 0142 UTC (Figures 2 and 10). Most 15-day backward trajectories originate over the northeast Pacific Ocean (Figure 11b). The parcels travel southeast near the North American coast heading toward the equator. Although this route generally is similar to that of Plume 1's trajectories (Figure 11a), many more of Plume 1's trajectories reach the Asian continent within 15 days. Regression diagrams for the plume are

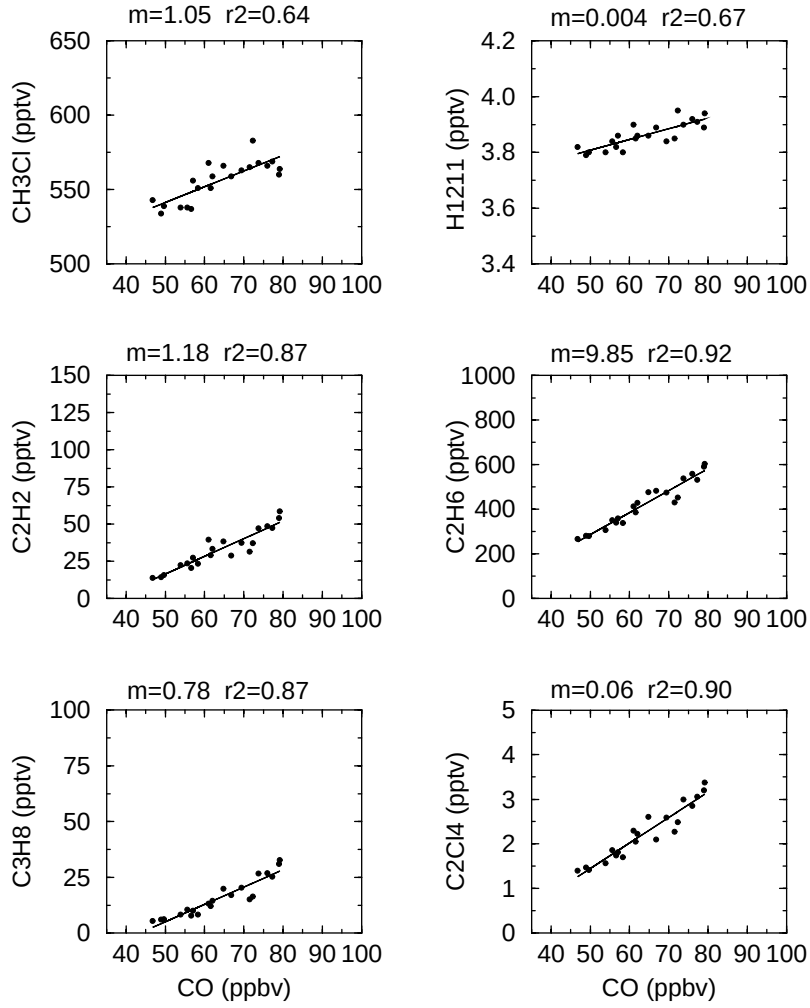

Figure 12. Correlation plots for Plume 2 of DC-8 Flight 9 for CH_3Cl (pptv), Halon-1211 (pptv), C_2H_2 (pptv), C_2H_6 (pptv), C_3H_8 (pptv), and C_2Cl_4 (pptv) versus CO (ppbv). Linear regressions are shown for each correlation. The slopes (m) of the regressions represent the enhancement ratios.

shown in Figure 12. It should be noted that points comprising the plots come from both the low level run and the bracketing higher altitudes during the climb-out (i.e., between the dotted vertical lines in Figure 10). These higher altitude points had to be included to obtain a sufficiently wide range of values. Results show that the various tracer species are well correlated with CO (r^2 ranges from 0.64 to 0.92).

[45] Plume 3 of DC-8 Flight 9, sampled during the third low level run from 0310 to 0330 UTC (Figures 2 and 10), is located southwest of the previous two plumes. Since wind speeds in the tropics are much slower than in the middle latitudes, the lengths of Plume 3's backward trajectories are relatively short (Figure 11c). However, most have 15-day origins over the north-east Pacific Ocean, and their paths are consistent with those of the previous plumes. Although no trajectories reach Asia within 15 days, we hypothesize that they would do so if the computational period were extended. Thus, we believe that Plume 3 represents another sample of the ''river.''

[46] Plume 4 is the last in the series of low-level sampling runs during DC-8 Flight 9, occurring between 0445 and 0505 UTC (Figures 2 and 10). By this point, the chemical signatures in the time series (Figure 10) have diminished considerably from those of Plume 1. Trajectories show that the 15-day origins cover a wide range of latitudes over the eastern tropical Pacific (Figure 11d). Many trajectories extend back to the Northern Hemisphere, and based on results of the previous plumes, we hypothesize that many of them ultimately originated over Asia and farther west. On the other hand, other trajectories remain in the Southern Hemisphere during the entire 15 day period. Based on large scale flow patterns (not shown), we believe that these trajectories would remain in the Southern Hemisphere if the period were extended beyond 15 days, possibly recurving from the west. Thus, Plume 4 appears to have a southern hemispheric influence.

[47] Correlations for Plume 4 (Figure 13) are strong ($r^2 > 0.70$) for all species except propane (C_3H_8) ($r^2 = 0.31$), which is reduced to the local background. This decrease probably is due to propane's relatively short lifetime in the equatorial boundary layer (7–16 days, Table 1). Except for CH_3Cl, slopes of the well-correlated species in Plume 4 generally are considerably less than those of Plume 2

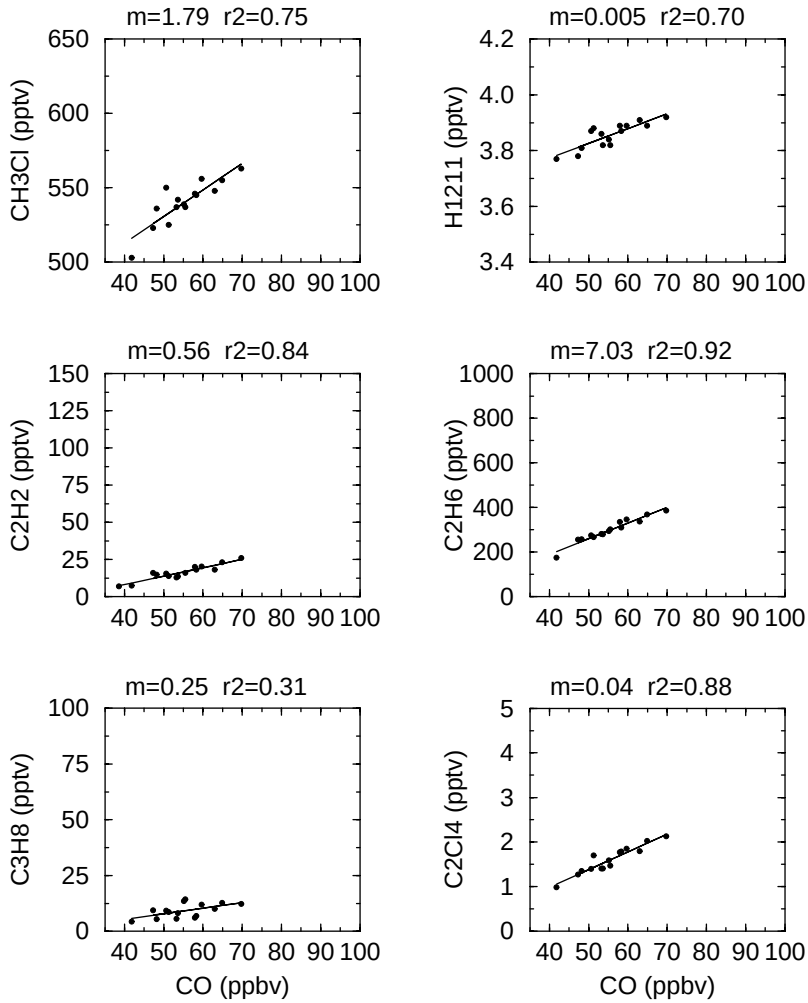

Figure 13. Correlation plots for Plume 4 of DC-8 Flight 9 for CH_3Cl (pptv), Halon-1211 (pptv), C_2H_2 (pptv), C_2H_6 (pptv), C_3H_8 (pptv), and C_2Cl_4 (pptv) versus CO (ppbv). Linear regressions are shown for each correlation. The slopes (m) of the regressions represent the enhancement ratios.

(Figure 12). This is consistent with both Plume 4's greater age from its likely Asian/European sources and the influence of the Southern Hemisphere.

[48] One should note that the regression slope for CH_3Cl is greater for Plume 4 than Plume 2 (1.79 versus 1.05, Figures 12 and 13). This occurs because CO decreases with each successive boundary layer run, whereas CH_3Cl remains relatively constant (Figure 10). CH_3Cl has a much longer lifetime than CO (Table 1); so this behavior is also consistent with photochemical aging.

[49] To summarize, transit times from the coast of Asia to Plume 1 are between 12 and 15 days, and are estimated to be 17 to 20 days for Plume 4. The slow, southwestward movement through the deep tropics is associated with photochemical processing and dilution that is evident in both the time series of chemical species and in correlations with CO. We next examine a final flight that is at the western end of the "river of pollution."

3.4. DC-8 Flight 11, Fiji Local No. 2

[50] DC-8 Flight 11 is the western most track plotted in Figure 2. It was the second local mission from Fiji (17.9°S, 176.9°E), heading northwest at 2117 UTC 22 March 1999. At 0110 UTC, at its westernmost extent near coastal New Guinea, the aircraft began descending into the marine boundary layer. The time series (Figure 14) shows only a slight enhancement in CO above the local background, with the maximum value of 59.9 ppbv indicating well aged air [*Talbot et al.*, 1996]. We will consider this period of slightly enhanced CO to be a weak plume even though CO is only ~15 ppbv greater than the local (higher altitude) background, not the 20 ppbv required previously.

[51] Other tracers also show little or no enhancement in the plume (Figure 14). There is a slight increase in long-lived ethane (C_2H_6), ~125 pptv above the local background. However, the industrial species C_2Cl_4 is only ~0.5 pptv greater than its background, and shorter lived propane (C_3H_8) shows no enhancement and sometimes even drops to its limit of detection. There is little indication of enhanced ethyne (C_2H_2), and fluctuations in CH_3Cl and Halon-1211 also are near background. Clearly, this plume exhibits the smallest mixing ratios of any plume described previously, indicating well aged, greatly diluted air.

[52] The 15-day backward trajectories for the Flight 11 plume (Figure 15) show that most parcels originate in the Northern Hemisphere over the eastern tropical Pacific. They

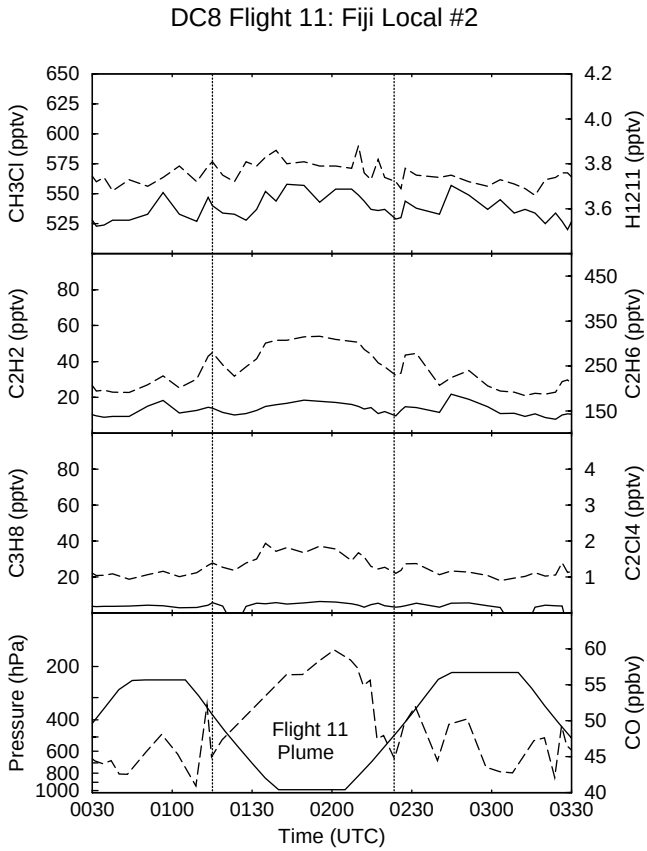

Figure 14. Time series of CH_3Cl (pptv), Halon-1211 (pptv), C_2H_2 (pptv), C_2H_6 (pptv), C_3H_8 (pptv), C_2Cl_4 (pptv), aircraft altitude (hPa), and CO (ppbv) along a portion of DC-8 Flight 11. The single plume encountered on this flight lies between the dotted vertical lines. Values corresponding to the left ordinate axes are plotted with a solid line; a dashed line corresponds to values on the right ordinate axes.

follow a slow southwestward route due to the northeasterly trade winds. The trajectories begin at relatively low levels and continue to descend. No continental source is indicated during the period. Since 15-day origins are near the arrival points of the backward trajectories calculated for P-3B Flight 4 (Figure 4) and are consistent with trajectories for the other flights, we believe that this plume also is part of the "river."

[53] *Jaffe et al.* [1997] observed fluctuations in CO at Guam (13°N, 145°W) that were associated with ten-day backward trajectories that moved slowly toward Guam from the east in, or near, the boundary layer. The origins of the CO were unknown since the trajectories did not pass over any appreciable landmass during the ten day period (their Figure 5f). Their trajectories are consistent with those shown here (Figures 4, 9, 11, and 15), i.e., long-range transport from Asia and even farther west.

4. Discussion

[54] We believe that the meteorological and chemical data from the four flights just described form a consistent picture of the "river of pollution" during PEM T-B. For example,

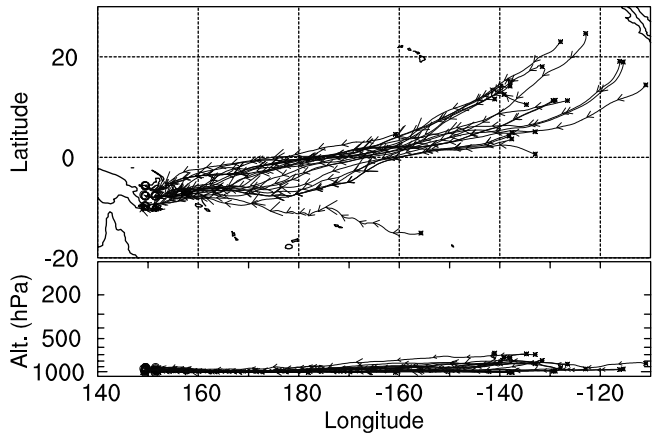

Figure 15. Clusters of 15-day backward trajectories arriving at the single plume of DC-8 Flight 11. The trajectories arrive at 0000 UTC 23 March 1999.

the "river" appears clearly in the composite of backward trajectories from the various plumes described earlier (Figure 16). For the sake of clarity, only the center flight-level trajectory of each second or third cluster has been plotted. Pollutants leaving Asia in the middle and upper troposphere are transported rapidly across the Pacific by the midlatitude westerly winds. As parcels reach the eastern Pacific, they turn southeast and descend in response to the subtropical anticyclone. The higher altitude/higher latitude parcels of P-3B Flight 4 Plume 1 then turn eastward (not shown here, but seen in Figure 7). However, the lower altitude/lower latitude parcels continue south along the North American coast where they may receive additional chemical input. They then veer southwest due to the northeasterly trade winds that dominate the tropics. Additional sources from Central and South America can be considered tributaries of the river. Parcels ultimately traverse the tropical Pacific to near New Guinea. Typical transit times from Asia to this westernmost extreme are 20 to 25 days.

[55] Chemical measurements from the four flights show the changing chemical signatures at the various locations along the river. Figure 17 contains plots of boundary layer data (<1 km) from the previously described portions of P-3B Flights 4 and 17 and DC-8 Flights 9 and 11 that

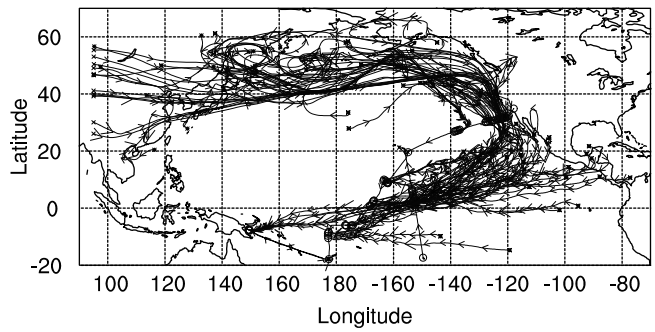

Figure 16. Backward trajectories from the four study flights that map the hypothesized "river of pollution." Plume 1 of P-3B Flight 4 is not shown. The four flight tracks are indicated.

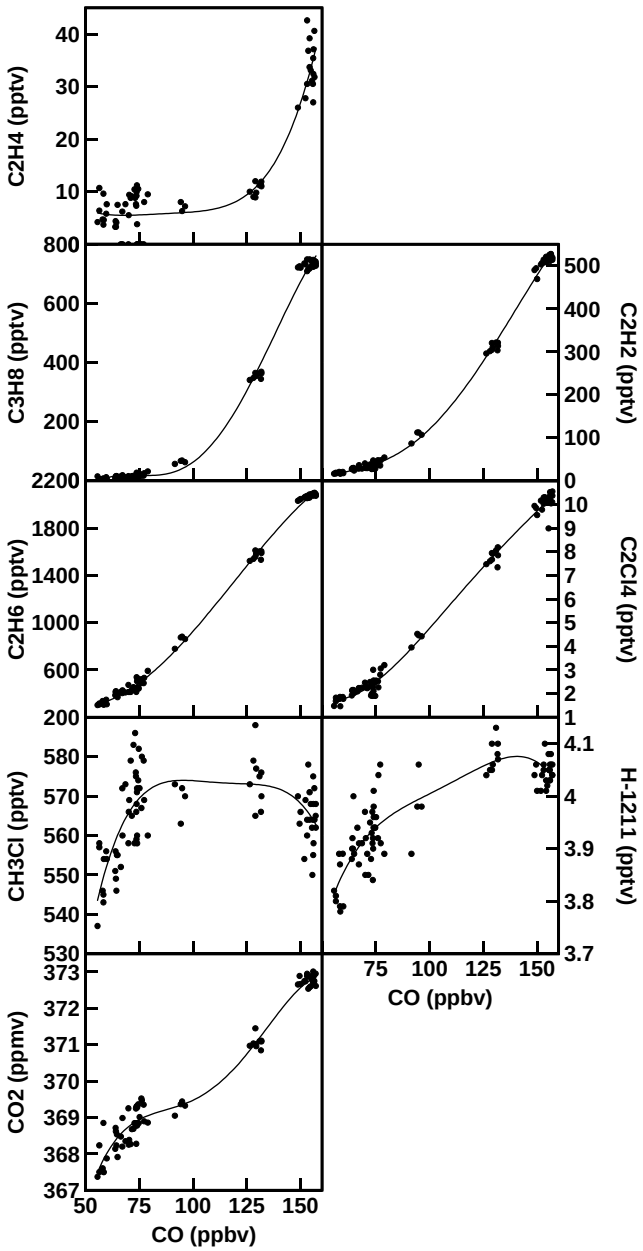

Figure 17. Plots of tracer species versus CO (ppbv) for boundary layer runs (<1 km) examined during the four flights. Plume 1 of P-3B Flight 4 is not included. Tracer species are C_2H_4 (pptv), C_3H_8 (pptv), C_2H_2 (pptv), C_2H_6 (pptv), C_2Cl_4 (pptv), CH_3Cl (pptv), Halon-1211 (pptv), and CO_2 (ppmv). Fourth order polynomial trend lines are superimposed.

comprise the river. Plume 1 of Flight 4 has excluded (as done in Figure 16) since that air did not head southwestward into the tropics. The panels are arranged according to the lifetimes of the various species (Table 1). The line that is superimposed on each panel represents a simple fourth-order polynomial fit to help reveal trends in the data.

[56] Using the plot for ethene (C_2H_4, Figure 17) as an example, the cluster of points in the upper right represents Plume 2 of P-3B Flight 4, with the next cluster representing Plume 3 of the same flight, followed by Plume 1 of DC-8 Flight 9. The large cluster of points in the lower left corresponds to P-3B Flight 17 and the remaining plumes of DC-8 Flight 9, with the points in the extreme lower left being from DC-8 Flight 11. The plot for ethene shows a well-defined trend, with values decreasing rapidly due its brief photochemical lifetime. Photochemistry also contributes to the accelerated losses of propane (C_3H_8) and ethyne (C_2H_2). Since lifetimes of ethane (C_2H_6) and C_2Cl_4 are most similar to that of CO (Table 1), their behavior is closest to being linear with CO. As noted earlier, dilution also contributes significantly to the decrease in each species with time.

[57] Qualitatively, the behavior in CO_2 (Figure 17) is consistent with what might be expected from an inert tracer. Since the evolution of CO arises from a combination of photochemistry and dilution, its enhancements above background values decay more rapidly than enhancements of CO_2 which are removed exclusively by mixing. This is exhibited by the bend in the trend line for CO_2 across the data sparse region between 75 and 125 ppbv of CO. The reduction in the CO_2 enhancement across this region is proportionally smaller due to the lack of a photochemical contribution to its loss. Unfortunately, it is difficult to examine this relationship more quantitatively without specific information about mixing rates and background concentrations being mixed with these enhanced values of CO and CO_2.

[58] The plots for Halon-1211 and methyl chloride (CH_3Cl) (Figure 17) are not consistent with what might be expected from an inert tracer. The precision of the halocarbon measurements [*Colman et al.*, 2001] indicates that the trends are significant. However, we can only speculate as to the causes for the observed distributions. The rapid decrease in Halon-1211 at low CO (<75 ppbv) is most likely due to the dilution of northern hemispheric air with southern hemispheric air along the inter-hemispheric gradient. Mean values during the PEM T-B period (Table 2) [see also *Blake et al.*, 2001] show that southern hemispheric air contains smaller mixing ratios in both altitude ranges. Trajectories from P-3B Flight 17 (Figure 9), Plume 4 of DC-8 Flight 9 (Figure 11d), and DC-8 Flight 11 (Figure 15)

Table 2. Mean Mixing Ratios for the Entire PEM T-B Period for Three Latitude Regions of the Remote Pacific[a]

Ethane	Ethyne	Propane	C_2Cl_4	CH_3Cl	H-1211	CO	CO_2
			Latitudes >10°N				
2–8 km							
808	145	85	3.6	579	4.04	97	368.9
0–2 km							
1316	264	276	6.7	571	4.07	120	370.2
			Latitudes 10°N–5°S				
2–8 km							
381	29	15	2.0	550	3.86	61	367.8
0–2 km							
470	38	20	2.6	565	3.90	74	368.8
			Latitudes >10°S				
2–8 km							
240	15	6	1.2	536	3.77	48	366.3
0–2 km							
185	11	5	1.1	527	3.72	44	365.6

[a] Values are in parts per trillion by volume (pptv), except for CO, which is in parts per billion (ppbv), and CO_2, which is in parts per million (ppmv).

show a southern hemispheric influence. It also should be noted that of the gases examined, methyl chloride (CH_3Cl) and Halon-1211 have more heterogeneous source distributions that may lead to greater variability in their relationship with CO.

[59] Vertical mixing also may be a factor in explaining the delayed decrease of methyl chloride (CH_3Cl) and Halon-1211 in Figure 17 since Table 2 displays greater values of methyl chloride aloft in the northern latitude range. Halon-1211 is only slighter smaller, while the other gases show significantly smaller average mixing ratios above 2 km. Finally, it should be noted that CH_3Cl has an oceanic source that may be important at long distances from land-based sources. *Khalil et al.* [1999] stated that the oceanic source is ~12% of the total budget; however, flux measurements suggest that the ocean could add approximately 2–10 pptv per day near the equator, depending on the height of the marine boundary layer and other factors.

[60] Figure 18 contains plots for the four plumes encountered during DC-8 Flight 9, where the solid circles denote Plume 1, open circles Plume 2, solid squares Plume 3, and open squares Plume 4. The lifetime of ethene (C_2H_2) is very short (Table 1) compared to the travel time from its apparent Asian source. Thus, the trend in Figure 18 is somewhat surprising. The plots of Halon-1211 and methyl chloride (CH_3Cl) again exhibit complex distributions that are difficult to explain (see previous discussion). Trends for most of the other species are similar to those seen in Figure 17 for the composite of flights, e.g., propane (C_3H_8), ethyne (C_2H_2), ethane (C_2H_6), C_2Cl_4, and CO_2. Thus, the chemical data for Flight 9 appear to be consistent with the trajectory data in Figure 11, showing that Plumes 1 through 4 represent a progressive aging and dilution along the river of pollution.

5. Summary and Conclusions

[61] We have investigated the hypothesis that a "river like" transport mechanism carried pollutants from Asia (and locations farther west) to the equatorial Pacific during the second Pacific Exploratory Mission to the Tropics (PEM T-B, February to April 1999). Specifically, pollution was rapidly transported across the North Pacific by middle latitude westerly winds, wrapped around the subtropical anticyclone and subsided, and finally carried southwestward by the low-level northeasterly easterly trade winds to the western tropical Pacific.

[62] We examined four flights from PEM T-B that sampled this hypothesized "river" at different points along its length. Thus, our approach was non-Lagrangian, i.e., we did not follow the same parcels along this entire journey. Chemical species used to assess the age and characteristics of observed pollution signatures included CO, methyl chloride (CH_3Cl), Halon-1211, ethyne (C_2H_2), ethene (C_2H_4), ethane (C_2H_6), perchloroethylene (C_2Cl_4), and propane (C_3H_8). Chemical plumes were defined based on the enhancement of CO relative to its local background which sometimes was at higher altitudes. Kinematic trajectories were calculated along the flight tracks using ECMWF global meteorological data. These trajectories represented the transport paths that air parcels experienced in route to (backward trajectories) or away from (forward trajectories) the selected flight tracks.

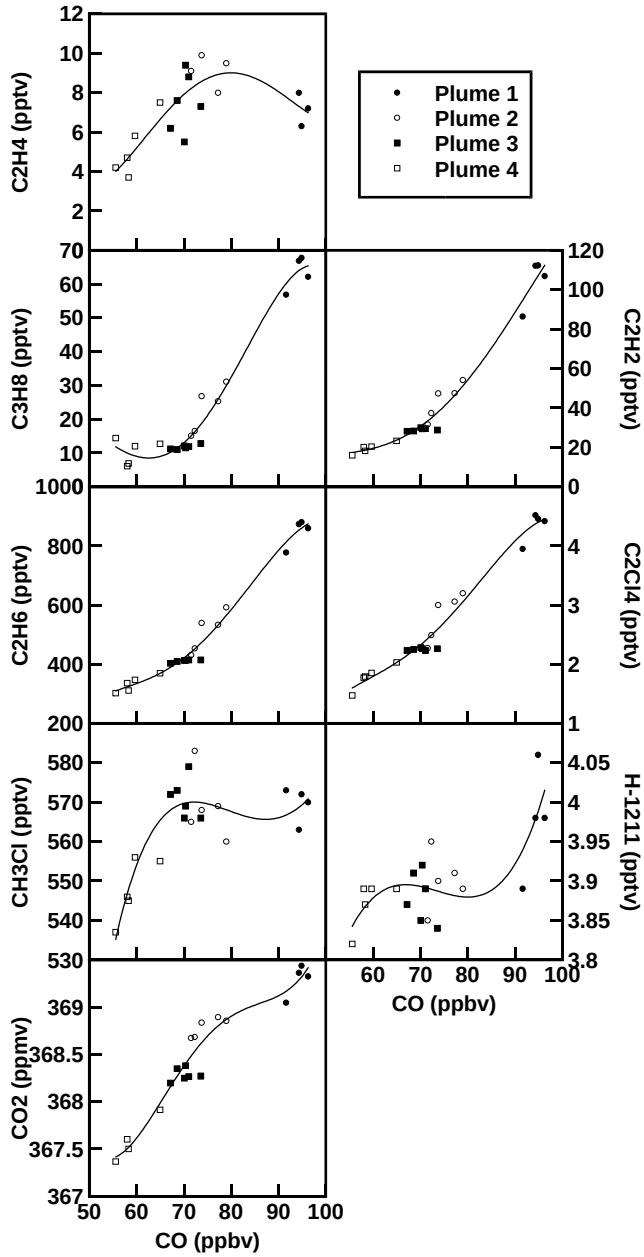

Figure 18. Plots of tracer species versus CO (ppbv) for the four boundary layer runs (<1 km) of DC-8 Flight 9. The various symbols denote Plume 1, Plume 2, Plume 3 and Plume 4. Tracer species are C_2H_4 (pptv), C_3H_8 (pptv), C_2H_2 (pptv), C_2H_6 (pptv), C_2Cl_4 (pptv), CH_3Cl (pptv), Halon-1211 (pptv), and CO_2 (ppmv). Fourth order polynomial trend lines are superimposed.

[63] Three plumes just southwest of California were examined first (during P-3B Flight 4). One plume was encountered in the middle troposphere, while the other two were observed in the marine boundary layer. The higher altitude plume exhibited a strong biomass burning influence, while the lower level plumes exhibited a predominantly industrial influence. Backward trajectories showed that the middle tropospheric plume experienced rapid upper level transport, extending to southeast Asian sources of biomass burning. Conversely, the two lower altitude plumes

had followed a less coherent path over industrialized northeastern Asia across the North Pacific. Forward trajectories showed that parcels comprising the upper level plume continued eastward toward North America. Conversely, parcels of the lower level plumes headed southwestward toward the eastern tropical Pacific.

[64] Plumes encountered during the three PEM T-B flights in the tropics showed greatly reduced chemical signatures compared to those sampled during the first just described. Both the trajectories and chemical data suggested that these tropical plumes were successively farther downstream from the coast of Asia. For example, backward trajectories from the plume examined near 5°N, 155°W (during P-3B Flight 17 from Tahiti to Hawaii) had passed over northern Asia with transit times from the continent being 10–15 days. The trajectories also indicated "tributaries" from the Americas.

[65] Four low altitude plumes were examined during the third flight of the series (DC-8 Flight 9 from Hilo to Fiji). These plumes exhibited a successive reduction in trace gas concentrations as the flight continued southwestward. Backward trajectories from plumes sampled along the southwest portion of Flight 9 had longer transit paths from their continental source than did plumes along the northeast portion of the flight. These longer paths are consistent with the steady degradation seen in the plumes' chemical signatures as they were sampled deeper over the tropical Pacific.

[66] The western most plume that we examined was encountered just east of New Guinea during DC-8 Flight 11. Mixing ratios of chemical species comprising this plume had degraded to near background levels, i.e., smaller than those of plumes described earlier. Backward trajectories showed a long, slow, southwestward progression across the tropical Pacific with no continental influence during the 15-day period. We believe that these trajectories had passed over Asia approximately three weeks earlier.

[67] These results document a type of global scale atmospheric transport that occurred during the northern hemispheric late winter and early spring of 1999. The transport is a long, slow process that spans the entire North Pacific Basin, carrying emissions from Asia (and beyond) toward the boundary layer of the equatorial Pacific. Documenting the delivery of middle latitude pollution to the tropics is important since tropical conditions lead to more efficient processing of pollution. The abundant sunlight and high humidity accelerate the loss of photochemically sensitive species, and the increased vertical mixing due to convective activity leads to more rapid mixing of longer-lived species into the background atmosphere.

[68] Although further research is needed to determine whether this transport occurs frequently, climatological wind charts suggest that the "river's flow pattern" is a common occurrence during Spring. However, the middle and upper tropospheric pollutant transport from Asia (and beyond) probably is episodic. This is because the processes transporting pollutants from the surface to these higher levels are episodic, e.g., frontal lifting, deep convection, etc. Thus, there will be fluctuations in the amount of pollution carried by the "river" as it departs Asia. Since considerable mixing and dilution occur during the several week transit to the boundary layer equatorial Pacific, the sharp gradients associated with the episodes leaving Asia are greatly reduced. Although we did not detect episodic pulses of pollution during our limited number of flights in the equatorial boundary layer, we do not rule them out. In fact, as noted earlier, *Jaffe et al.* [1997] did observe pollution events over Guam that seem to be explained by our long-range transport scenario.

[69] Since wind currents in the Southern Hemisphere are a mirror image of those farther north (e.g., Figure 1), it is likely that a corresponding "river of pollution" also exists in that hemisphere. Such transport could carry pollutants from biomass burning over southern Africa and South America eastward where they would recurve due to the southern hemispheric subtropical anticyclone and be carried back westward by the trade winds. Thus, these aged parcels from southern hemispheric biomass burning could be juxtaposed with northern hemispheric aged parcels from Asia. Future studies should examine this hypothesis, perhaps using data from NASA's first Pacific Exploratory Mission to the Tropics which was conducted during the southern hemispheric burning season [e.g., *Hoell et al.*, 1999; *Fuelberg et al.*, 1999]. Such studies should include both diagnostic and chemical transport modeling components.

[70] **Acknowledgments.** We appreciate the assistance of several students at Florida State University who helped with this research. They include Chris Kiley, John Hannan, Joe Maloney, and Greg Quina. The research was funded by NASA's Tropospheric Chemistry Program through Grant NCC-1-308 to Florida State University under the auspices of the Langley Research Center. The thoughtful suggestions of the reviewers helped clarify portions of the text.

References

Angevine, W. M., M. Trainer, S. A. McKeen, and C. M. Berkowitz, Mesoscale meteorology of the New England coast, Gulf of Maine, and Nova Scotia, *J. Geophys. Res.*, *101*, 28,893–28,902, 1996.

Bernsten, T. K., S. Karlsdottir, and D. A. Jaffe, Influence of Asian emissions on the composition of air reaching the north western United States, *Geophys. Res. Lett.*, *26*, 2171–2174, 1999.

Blake, D. R., and F. S. Rowland, Urban leakage of liquefied petroleum gas and its impact on Mexico City air quality, *Science*, *269*, 953–956, 1995.

Blake, D. R., T. Chen, T. Smith Jr., C. Wang, O. Wingenter, N. J. Blake, F. S. Rowland, and E. Mayer Three-dimensional distribution of nonmethane hydrocarbons and halocarbons over the northwestern Pacific during the 1991 Pacific Exploratory Mission (PEM-West A), *J. Geophys. Res.*, *101*, 1763–1778, 1996.

Blake, N. J., et al., Influence of southern hemispheric biomass burning on nonmethane hydrocarbons and selected halocarbons over the remote South Pacific, *J. Geophys. Res.*, *104*, 16,213–16,232, 1999.

Blake, Nicola J., et al., Large-scale latitudinal and vertical distributions of NMHCs and selected halocarbons in the troposphere over the Pacific Ocean during the March–April 1999 Pacific Exploratory Expedition (PEM-Tropics-B), *J. Geophys. Res.*, *107*(D23), 32,627–32,644, 2001.

Clarke, A., W. Collins, P. Rasch, V. Kapustin, K. Moore, S. Howell, and H. Fuelberg, Dust and pollution transport on global scales: Aerosol measurements and model predictions, *J. Geophys. Res.*, *106*(D23), 32,555–32,569, 2001.

Colman, J. J., A. L. Swanson, S. Meinardi, B. C. Sive, and D. R. Blake, Description of the analysis of a wide range of volatile organic compounds in whole air samples collected during PEM-Tropics A and B, *Anal. Chem.*, *73*, 3723–3731, 2001.

Crawford, J., et al., Evolution and chemical consequences of lightning produced NO_x observed in the North Atlantic upper troposphere, *J. Geophys. Res.*, *105*, 19,795–19,809, 2000.

Doty, K. G., and D. J. Perkey, Sensitivity of trajectory calculations to the temporal frequency of wind data, *Mon. Weather Rev.*, *121*, 387–401, 1993.

European Centre for Medium-Range Weather Forecasts (ECMWF), *User Guide to ECMWF Products 2.1*, *Meteorol. Bull. M3.2*, Reading, UK, 1995.

Fraser, P. J., D. E. Oram, C. E. Reeves, S. A. Penkett, and A. McCulloch,

Southern Hemispheric halon trends and global halon emissions, *J. Geophys. Res.*, *104*, 15,985–15,999, 1999.

Fuelberg, H. E., R. O. Loring Jr., M. V. Watson, M. C. Sinha, K. E. Pickering, A. M. Thompson, G. W. Sachse, D. R. Blake, and M. R. Schoeberl, TRACE A trajectory intercomparison, 2, Isentropic and kinematic methods, *J. Geophys. Res.*, *101*, 23,927–23,939, 1996.

Fuelberg, H. E., R. E. Newell, S. P. Longmore, Y. Zhu, D. J. Westberg, E. V. Browell, D. R. Blake, G. L. Gregory, and G. W. Sachse, A meteorological overview of the Pacific Exploratory Mission (PEM) Tropics period, *J. Geophys. Res.*, *104*, 5585–5622, 1999.

Fuelberg, H. E., J. R. Hannan, P. F. J. van Velthoven, E. V. Browell, G. Bieberbach Jr., R. D. Knabb, G. L. Gregory, K. E. Pickering, and H. B. Selkirk, A meteorological overview of the SONEX period, *J. Geophys. Res.*, *105*, 3633–3651, 2000.

Fuelberg, H. E., R. E. Newell, D. J. Westberg, J. C. Maloney, J. R. Hannan, B. D. Martin, M. A. Avery, and Y. Zhu, A meteorological overview of the second Pacific Exploratory Mission in the Tropics, *J. Geophys. Res.*, *106*(D23), 32,427–32,443, 2001.

Garstang, M., P. D. Tyson, R. Swap, M. Edward, P. Kallberg, and A. J. Lindesay, Horizontal and vertical transport of air over southern Africa, *J. Geophys. Res.*, *101*, 23,721–23,736, 1996.

Gregory, G. L., J. T. Merrill, M. C. Shipham, D. R. Blake, G. W. Sachse, and H. B. Singh, Chemical characteristics of tropospheric air over the Pacific Ocean as measured during PEM-West B: Relationship to Asian outflow and trajectory history, *J. Geophys. Res.*, *102*, 28,275–28,285, 1997.

Hannan, J. R., et al., Atmospheric chemical transport based on high-resolution model-derived winds: A case study, *J. Geophys. Res.*, *105*, 3807–3820, 2000.

Hoell, J. M., D. D. Davis, D. J. Jacob, M. O. Rogers, R. E. Newell, H. E. Fuelberg, R. J. McNeal, J. L. Raper, and R. J. Bendura, Pacific Exploratory Mission in the tropical Pacific: PEM-Tropics A, August–September 1996, *J. Geophys. Res.*, *104*, 5567–5583, 1999.

Jacob, D. J., J. A. Logan, and P. P. Murti, Effect or rising Asian emissions on surface ozone in the United States, *Geophys. Res. Lett.*, *26*, 2175–2178, 1999.

Jaffe, D., A. Mahura, J. Kelley, J. Atkins, P. C. Novelli, and J. Merrill, Impact of Asian emissions on the remote North Pacific atmosphere: Interpretation of CO data from Shemya, Guam, Midway, and Mauna Loa, *J. Geophys. Res.*, *102*, 28,627–28,635, 1997.

Jaffe, D., et al., Transport of Asian air pollution to North America, *Geophys. Res. Lett.*, *26*, 711–714, 1999.

Kahl, J. D., A cautionary note on the use of air trajectories in interpreting atmospheric chemistry measurements, *Atmos. Environ., Part A*, *27*, 3037–3038, 1993.

Kaneyasu, N., K. Takeuchi, M. Hayashi, S. Fujita, I. Uno, and H. Sasaki, Outflow pattern of pollutants from East Asia to the North Pacific in the winter monsoon, *J. Geophys. Res.*, *105*, 1761–1777, 2000.

Khalil, M. A. K., R. M. Moore, D. B. Harper, J. M. Lobert, D. J. Erickson, V. Koropalov, W. T. Sturges, and W. C. Keene, Natural emissions of chlorine-containing gases: Reactive chlorine emissions inventory, *J. Geophys. Res.*, *104*, 8333–8346, 1999.

Krishnamurti, T. N., H. E. Fuelberg, M. C. Sinha, D. Oosterhof, E. L. Bensman, and V. B. Kumar, The meteorological environment of the tropospheric ozone maximum over the tropical South Atlantic Ocean, *J. Geophys. Res.*, *98*, 10,621–10,641, 1993.

Maloney, J. C., H. Fuelberg, M. Avery, J. Crawford, D. R. Blake, B. Heikes, G. W. Sachse, S. Sandholm, H. Singh, and R. Talbot, Chemical characteristics of air from different source regions during the second Pacific Exploratory Mission in the Tropics (PEM-Tropics B), *J. Geophys. Res.*, *106*(D23), 32,609–32,625, 2001.

Mauzerall, D. L., J. A. Logan, D. J. Jacob, B. E. Anderson, D. R. Blake, J. D. Bradshaw, B. Heikes, G. W. Sachse, H. Singh, and B. Talbot, Photochemistry in biomass burning plumes and implications for tropospheric ozone over the tropical South Atlantic, *J. Geophys. Res.*, *103*, 8401–8423, 1998.

McKeen, S. A., S. C. Liu, E.-Y. Hsie, X. Lin, J. B. Bradshaw, S. Smyth, G. L. Gregory, and D. R. Blake, Hydrocarbon ratios during PEM-West A: A model perspective, *J. Geophys. Res.*, *101*, 2087–2109, 1996.

Merrill, J. T., Atmospheric long range transport to the Pacific Ocean, in *Chemical Ocenography*, vol. 10, edited by J. P. Riley and R. Duce, pp. 15–50, Academic, San Diego, Calif., 1989.

Merrill, J. T., R. Beck, and L. Avila, Modeling atmospheric transport to the Marshall Islands, *J. Geophys. Res.*, *90*, 12,927–12,936, 1985.

Montzka, S. A., J. H. Butler, J. W. Elkins, T. M. Thompson, A. D. Clarke, and L. T. Lock, Present and future trends in the atmospheric burden of ozone depleting halogens, *Nature*, *398*, 690–694, 1999.

Population Reference Bureau, Background: Asia and the Near East, 2000.

Raper, J. L., M. M. Kleb, D. J. Jacob, D. D. Davis, R. E. Newell, H. E. Fuelberg, R. J. Bendura, J. H. Hoell, and R. J. McNeal, Pacific Exploratory Mission in the Tropical Pacific: PEM-Tropics B, March–April 1999, *J. Geophys. Res.*, *106*(D23), 32,401–32,425, 2001.

Rasmussen, R. A., L. E. Rasmussen, M. A. K. Khalil, and R. W. Dalluge, Concentration distribution of methyl chloride in the atmosphere, *J. Geophys. Res.*, *85*, 7350–7356, 1980.

Riemer, D. D., P. J. Milne, R. G. Zika, and W. H. Pros, Photoproduction of nonmethane hydrocarbons (NMHCs) in seawater, *Mar. Chem.*, *71*, 177–198, 2000.

Simpson, J. E., *Sea Breeze and Local Winds*, 234 pp., Cambridge Univ. Press, New York, 1994.

Stohl, A., A 1-year Lagragian "climatology" of airstreams in the Northern Hemisphere troposphere and the lowermost stratosphere, *J. Geophys. Res.*, *106*(D7), 7263–7279, 2001.

Stohl, A., and P. Seibert, Accuracy of trajectories as determined from conservation of meteorological tracers, *Q. J. R. Meteorol. Soc.*, *124*, 1465–1484, 1998.

Stohl, A., and T. Trickl, A textbook example of long-range transport: Simultaneous observations of ozone maxima of stratospheric and North American origin in the free troposphere over Europe, *J. Geophys. Res.*, *104*, 30,445–30,462, 1999.

Stohl, A., G. Wotawa, P. Seibert, and H. Kromp-Kolb, Interpolation errors in wind fields as a function of spatial and temporal resolution and their impact on different types of kinematic trajectories, *J. Appl. Meteorol.*, *34*, 2149–2165, 1995.

Talbot, R. W., et al., Chemical characteristics of continental outflow over the tropical South Atlantic Ocean from Brazil and Africa, *J. Geophys. Res.*, *101*, 24,187–24,202, 1996.

Talbot, R. W., et al., Chemical characteristics of continental outflow from Asia to the troposphere over the western Pacific Ocean during February–March 1994: Results from PEM-West B, *J. Geophys. Res.*, *102*, 28,255–28,274, 1997.

United Nations Environment Programme (UNEP), *Handbook for the Montreal Protocol on Substances That Deplete the Ozone Layer*, 2nd ed., Ozone Secr., Nairobi, Kenya, 1991.

United Nations Environment Programme (UNEP), Nairobi, Kenya, Montreal protocol on substances that deplete the ozone layer, UNEP Technology and Economic Assessment Panel April 1999 Report, 1999.

Wernli, H., and H. C. Davies, A Lagragian-based analysis of extratropical cyclones, 1, The method and some applications, *Q. J. R. Meteorol. Soc.*, *123*, 467–489, 1997.

Wofsy, S. C., et al., Atmospheric chemistry in the Arctic and sub-Arctic: Influence of natural fires, industrial emissions, and stratospheric inputs, *J. Geophys. Res.*, *97*, 16,731–16,746, 1992.

D. R. Blake and N. J. Blake, University of California, Irvine, CA, USA.

J. H. Crawford and G. W. Sachse, NASA Langley Research Center, Hampton, VA, USA.

H. E. Fuelberg and B. D. Martin, Department of Meteorology, Florida State University, 404 Love Building, Tallahassee, FL 32306-4520, USA. (fuelberg@met.fsu.edu)

J. A. Logan, Harvard University, Cambridge, MA, USA.